EXPLORE
Newsletter for the
Association of Applied Geochemists
www.appliedgeochemists.org
NUMBER 183 JUNE 2019

Gold dispersion in transported cover sequences especially in chemical (palaeoredox front) and physical (unconformity) interfaces linked to the landscape history of Western Australia

Ravi Anand and Walid Salama, *CSIRO, Mineral Resources, 26 Dick Perry Avenue, Kensington WA 6151, Western Australia*

https://doi.org/10.70499/AEPM5129

Introduction

Transported cover is exotic or redistributed material of continental origin that blankets weathered and fresh bedrock, effectively obscuring bedrock-hosted mineralisation in many prospective areas. It includes unconsolidated to consolidated glacial, fluvio-glacial, colluvial-alluvial, lacustrine and estuarine sediments, evaporites and aeolian materials and several may occur in the sequence at a given site (Anand & Paine, 2002). In this paper, the term transported cover excludes marine, lithified sequences in sedimentary basins. Surficial sampling techniques have limited application in areas of deep transported cover. Many investigations have sought evidence for active dispersion through transported cover. In various locations, targeted sampling media such as termite mounds (e.g., Petts *et al*. 2009; Stewart *et al*. 2012; Stewart & Anand 2014), pedogenic carbonates (Lintern 2015), vegetation (e.g., Hill, 2004; Hulme & Hill 2005; Anand *et al*. 2007; Reid *et al*. 2008; Lintern *et al*. 2013a; Anand *et al*. 2016; Noble *et al*. 2017) have been shown to give a response through 2 to 20 m and rarely 30 m of transported cover in certain environments. Deep drilling through this cover to sample basement rocks is costly, yet the transported cover itself may provide an opportunity for exploration, due to geochemical dispersion from mineralisation into cover. If transported cover is to be a useful sample medium, indicator elements need to be dispersed into the cover during deposition and/or by post-depositional weathering and diagenesis. As older transported cover is more likely to contain elements that have been chemically dispersed from concealed mineralisation, the relative timing of continental sedimentation and the subsequent weathering events are important to understand for successful exploration. Older transported cover deposited during the Permian and Eocene-Miocene will have been subjected to more post-depositional alteration (and therefore trace element dispersion) than younger Quaternary transported cover such as recent colluvium and alluvium (Anand *et al*. 1993; Radford & Burton 1999; Butt *et al*. 2005; Hore & Hill 2009; Anand & Robertson 2012; Anand 2016; Salama *et al*. 2016a; Salama *et al*. 2018a,b; Baudet *et al*. 2018). In this paper, we will show how understanding metal dispersion in three transported cover settings (Permian, Eocene-Miocene and Quaternary) in Western Australia (Yilgarn Craton, Albany Fraser Orogen, Paterson Orogen) can be used to find buried gold deposits.

As it is impractical to sample the entire transported cover sequence, selective sampling is required. There are two types of interfaces that may be targeted to discover mineralisation (physical and chemical; Fig. 1), both of which are abundant and can be sampled from near-surface or by shallow drilling.

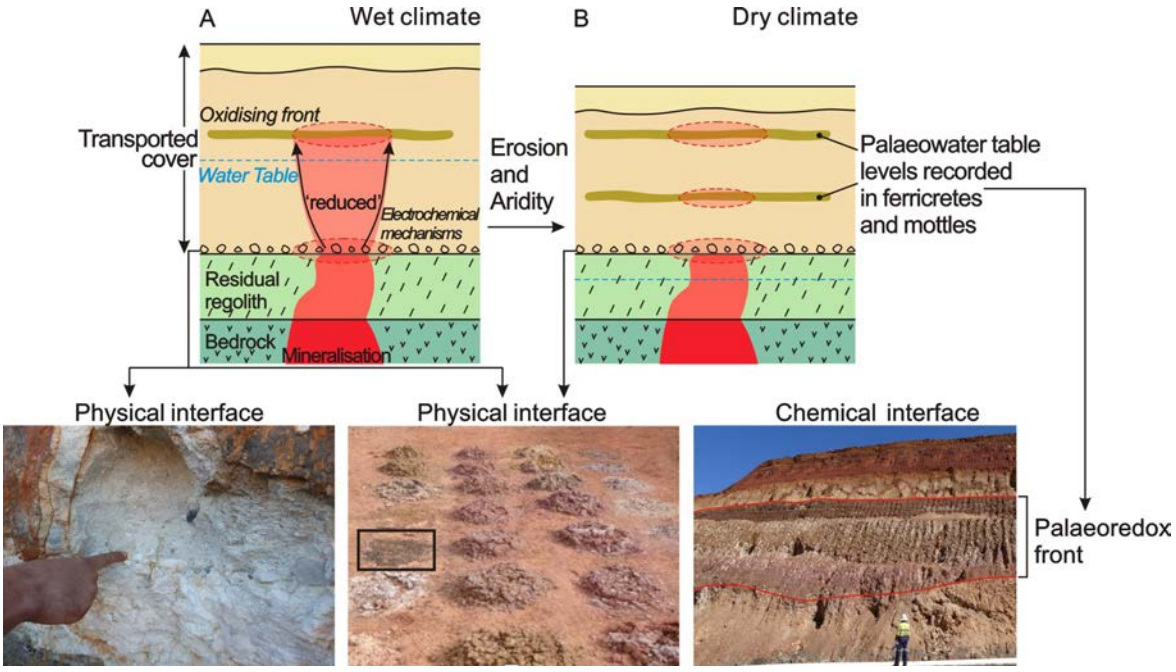

Figure 1. *Diagram and photos showing two types of interfaces (physical and chemical) in situ and in drill cuttings. Metal transfer in the regolith is driven by the influence of climate that disperses metals into chemical interfaces (modified after Anand et al. 2016). (A) A high water table within the transported cover, during an initial wet climate would allow electrochemical metal transfer to and adsorption onto redox materials (nodules, pisoliths, mottles). (B) Subsequent onset of aridity lowers the water table but the original anomalous zones remain.*

continued on page 5

Gold dispersion in transported cover sequences especially in… *continued from page 1*

Physical interface sampling is based on the possibility of dispersion at or close to an unconformity between the transported cover and the underlying rock by (i) mechanical dispersion of remnants of weathering, such as ferruginous duricrust, mineral grains, lithic and gossan fragments, and (ii) hydromorphic dispersion after deposition of the transported cover by groundwater percolating through the coarse, basal cover along the unconformity itself and/or the upper residual material (Anand *et al*. 1993; Robertson *et al*. 1996; Anand 2000; Robertson *et al*. 2001; Butt *et al*. 2005; Anand & Robertson 2012). These mechanisms result in lateral dispersions at the base of the cover, without upward dispersion. The base of the cover can be a simple, sharp, erosive unconformity or a complex mixture of saprolite and transported cover, a metre or more thick, possibly including a buried palaeosol. The extent of lateral dispersion is governed by the topography of the unconformity.

Chemical interface (palaeoredox fronts) sampling is based on hydromorphic dispersion into weathering products such as Fe and Mn oxides formed in transported cover when the water tables were higher. Although much of Australia is now semi-arid to arid, old transported cover (Permian; Eocene-Miocene) will have a long history of weathering under very different climates (discussed later). Transported cover across Australia can date back to the Permo-Carboniferous (Veevers 2000; Eyles & de Broekert 2001; Pillans 2005). Depending upon past climate and landscape positions, the water table could have been near the surface with connected saturation reaching from buried ore to the top of the water table (Fig. 1A). The development of a water table within transported cover sets up a redox gradient with oxidising conditions prevailing at and above the water table and reducing conditions below (Anand *et al*. 2016). The water table-associated Eh difference causes reduced ions (Fe^{2+}, Mn^{2+}) released from the weathering front to migrate upwards and oxidise at or near the water table (oxidation front), resulting in ferrolysis with the generation of acidic conditions at the oxidation front (Mann 1983). Thus, high water tables in wet climates are likely to electrochemically transfer metals into the cover across an Eh gradient (Fig. 1A; Anand *et al*. 2016). Anomalous zones are likely to be in water table-associated redox zones such as ferruginous nodules, pisoliths and mottles. These can be loose or cemented into a ferricrete. A shift to a drier climate coupled with erosion, would lower the water table generally to below the transported cover, but the old anomalous redox zone (Fe oxides) is likely to retain a geochemical signature of mineralisation (Fig. 1B; Anand *et al*. 2016).

Displaced anomalies can also form in transported cover sequences. For example, Zn and Cu concentrated in Fe and Mn oxides at redox fronts, may be derived by leaching from the transported cover, and be unrelated to any proximal basement mineralisation (Anand 2016). Such anomalies may be distinguished as false by regression analysis or by the absence of a multi-element signature – but with no certainty if the primary mineralisation itself lacks other elements, or only Cu and Zn have been mobilised. Conversely, the transported cover itself may have a high, multi-element background, or contain low grade mineralisation.

Geology

The Yilgarn Craton comprises an area of approximately 657,000 km^2 and forms one of the largest intact segments of the Archaean crust on Earth. Much of the Yilgarn Craton is a granite-greenstone terrain characterised by arcuate 'greenstone belts' of metamorphosed sedimentary and volcanic rocks that lie between large areas of granitoid rocks. The bulk of the Craton is thought to have formed between 3000 and 2600 Ma, with some gneissic terrains older than 3000 Ma in age (Myers 1993). The greenstones hosting orogenic gold mineralisation are ultramafic and mafic volcanic rocks formed as extensive submarine lavas, with local centres of felsic and mafic volcanic rocks.

The Albany Fraser Orogen is an arcuate Mesoproterozoic orogenic belt adjacent to the southern and southeastern margins of the Archaean Yilgarn Craton in Western Australia. It comprises two main tectonic units that reflects its relationship with the Yilgarn Craton: the Northern Foreland and the Kepa Kurl Booya Province. Northern Foreland consists of greenschist and amphibolite to granulite facies Archaean gneisses and granites. The Kepa Kurl Booya Province is defined as the crystalline basement of the Albany Fraser Orogen (Spaggiari *et al*. 2009).

The Paterson Orogen in Western Australia covers around 30 000 km^2 to the east of the Hamersley Basin and southwest

continued on page 6

Note: *This EXPLORE article has been extracted from the original EXPLORE Newsletter. Therefore, page numbers may not be continuous and any advertisement has been masked.*

Gold dispersion in transported cover sequences especially in… *continued from page 5*

of the Canning Basin. It consists of Early to Middle Proterozoic high grade metamorphic rocks, acid and basic intrusive rocks, shelf sediments and minor younger granite intrusive rocks. The region contains poorly exposed Neoproterozoic sedimentary successions in the northwest Paterson Orogen which are host to significant deposits of gold-copper, base metal and uranium (Bagas 2004).

Geochronology of weathering

In the Yilgarn Craton and the Albany Fraser and Paterson orogens of Western Australia, a deeply weathered mantle, many metres thick, is commonly overlain by transported cover of various ages. Although there is palaeomagnetic evidence for regolith ages as old as the Carboniferous on the Yilgarn Craton (Pillans 2005), glaciation in the Permian eroded most pre-existing regolith, leaving poorly consolidated transported cover that, in places, has since been weathered. Most of the preserved deeply weathered regolith has formed during the Late Cretaceous to Miocene (Anand & Paine 2002). Recently, there has been dating of ferruginisation of the deeply weathered mantle. Palaeomagnetic dating of hematite in weathering profiles from several locations in the Yilgarn Craton indicates two major periods of hematite formation (Pillans 2005; Anand & Robertson 2012). These include Maastrichtian to Palaeocene (60-75 Ma) and Late Miocene (10 Ma). (U-Th)/He dating of ferruginous nodules and pisoliths formed from the weathering of bedrock at the Garden Well gold deposit indicate an age of 15 Ma whereas ferruginous pisoliths formed in the Eocene-Miocene transported cover yield ages of 11-19 Ma (Anand, Wells & Salama, unpublished data). However, ferruginous pisoliths in the Darling Range of Western Australia are slightly younger as suggested by 10 -7.5 Ma (Pidgeon *et al*. 2004) and 5.7-1.3 Ma ages obtained by (U-Th)/He dating (Wells *et al*. 2018). Conditions were warm and humid from the Late Cretaceous to the end of the Early Miocene, with fluctuations to at least two cooler and drier episodes prior to the Oligocene (McGowran & Li 1998), when the vegetation was dominated by coniferous forests and woodlands. During the Late Miocene, a seasonally drier and warmer climate (though rainfall was still greater than at present; Martin 2006), occurred with consequent flora changes, as southern Australia drifted northwards. Thereafter, generally drier conditions prevailed. Thus, weathering profiles resulted from the overprinting by several climatic changes, including water table fluctuations, together with variations in salinity and groundwater residence times.

Transported cover classification

It is important to understand the nature of the transported cover and its influence on metal dispersion processes. There are broadly three principal transported sequences (Fig. 2; Anand & Paine 2002; Butt *et al*. 2005): Sequence

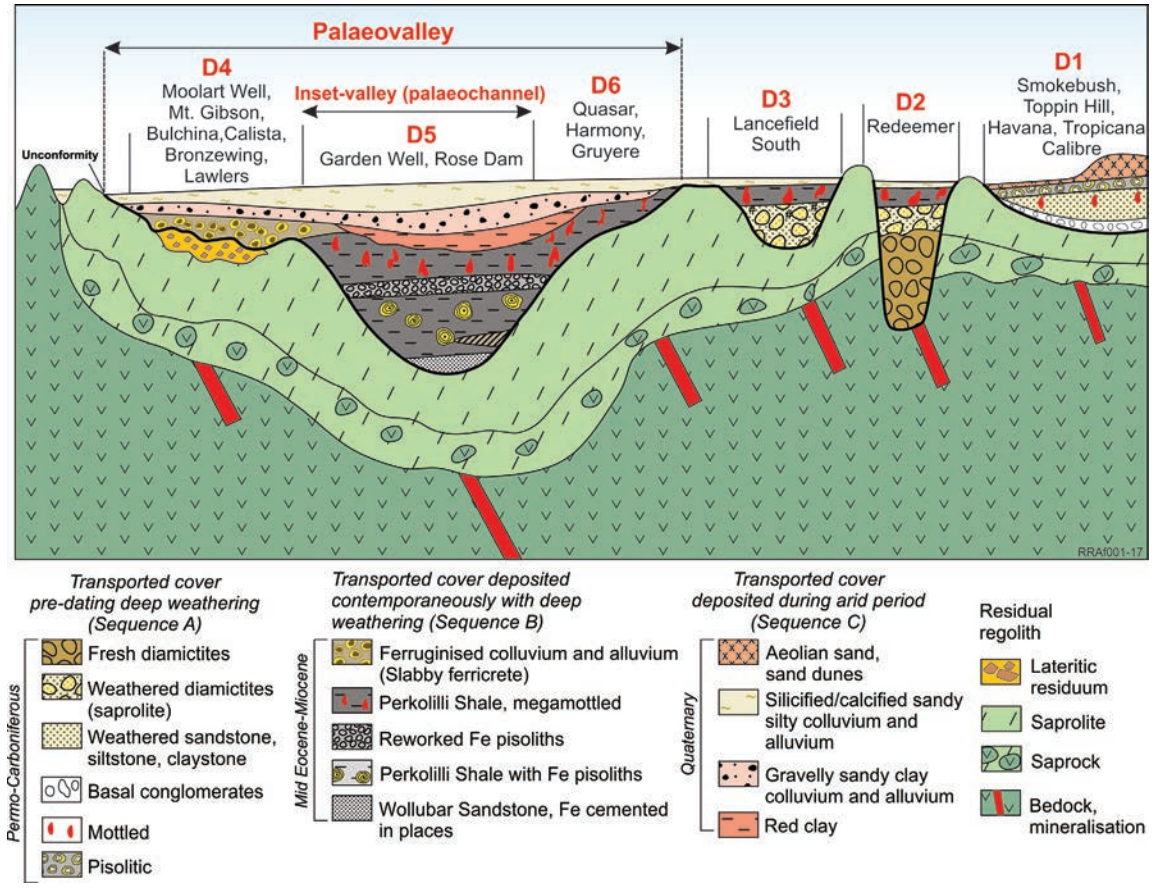

Figure 2. Classification and stratigraphy of some major transported cover units. D1-D6 represent different transported cover environments discussed in the text.

continued on page 8

Gold dispersion in transported cover sequences especially in… *continued from page 6*

A (*transported cover pre-dating deep weathering; Permo-Carboniferous), Sequence B (transported cover deposited contemporaneously with weathering; Mid Eocene-Miocene)* and *Sequence C (transported cover deposited during an arid period; Quaternary)*. These sequences can be further sub-divided according to the nature of the transported material (Fig. 2). In Western Australia, there has been post-depositional weathering and diagenesis of transported cover (Fig. 3). Older transported cover (Sequences A and B) is strongly ferruginised (goethite, hematite) as a result of wet-dry climatic changes during the Palaeocene and more commonly Miocene whereas transported cover of Sequence C, deposited in the arid period has been subjected to silicification, calcification and gypsification to form red-brown hardpan (silicified colluvium and alluvium), calcrete and gypcrete respectively (Anand 2005; Fig. 3). These principal transported cover sequences, briefly described below, are used as a framework for several case studies reported here from the Yilgarn Craton and the Albany Fraser and Paterson orogens of Western Australia (Fig. 4).

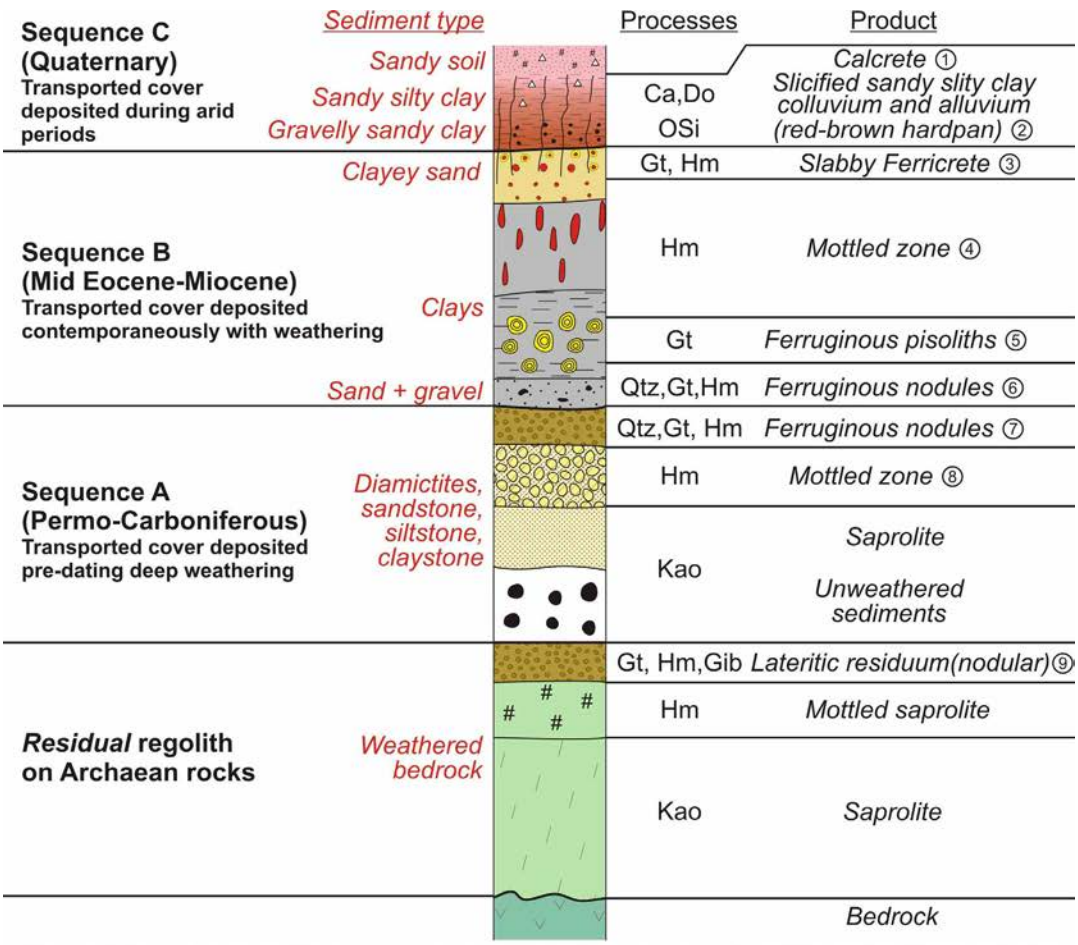

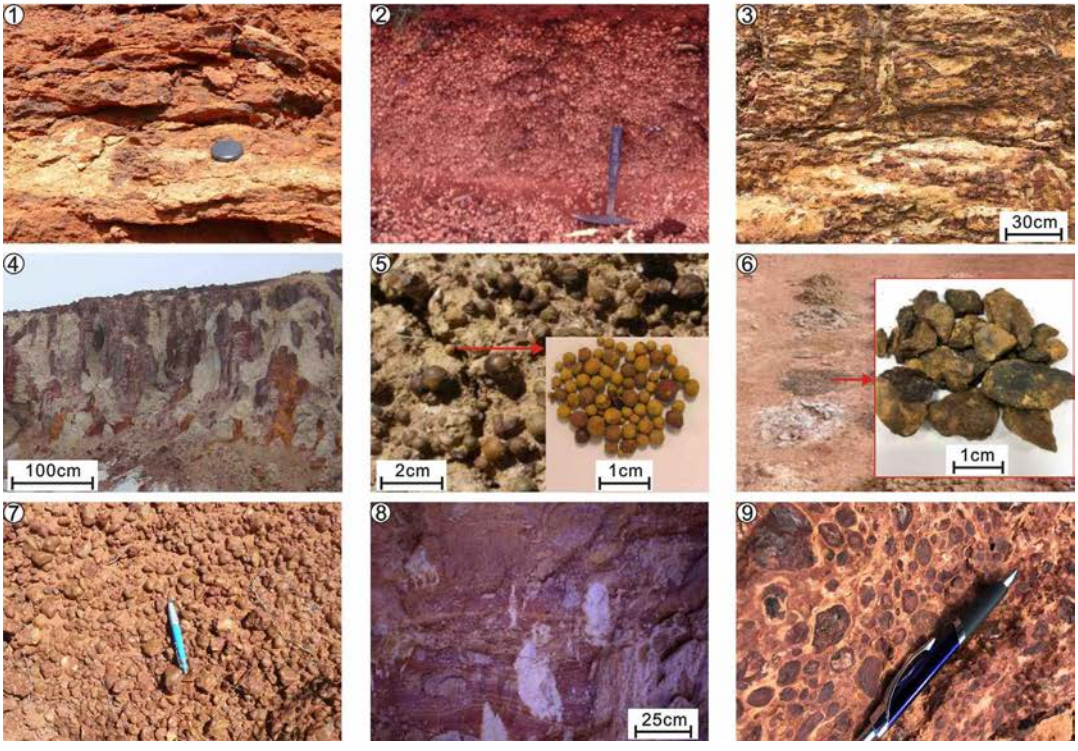

Figure 3. Post-depositional weathering and diagenetic features of transported cover units (modified after Anand 2005). 1 to 9 are photographs of some products that result from post-depositional weathering. See legend in Figure 2 for the different units.
Ca-calcite; Do=dolomite; OSi=Opaline silica; Gt=goethite; Hm=hematite; Qtz=quartz; Kao=kaolinite; Gib=gibbsite.

continued on page 9

Gold dispersion in transported cover sequences especially in… *continued from page 8*

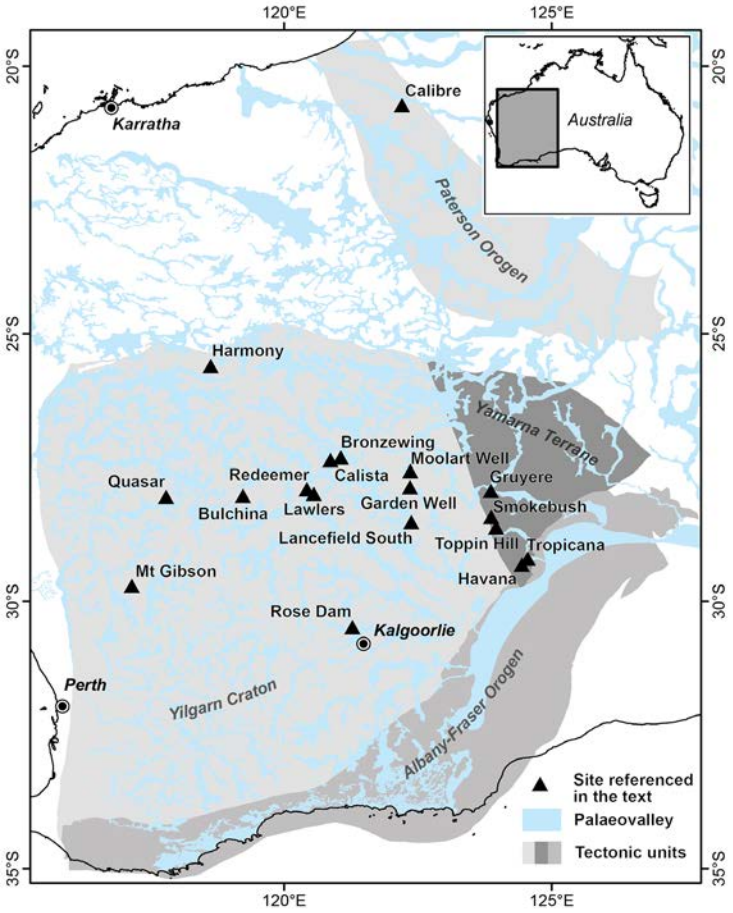

Figure 4. Location of the sites referred to in the text on Multi-resolution Valley Bottom Flatness (MrVBF) map (after Gallant & Dowling, 2003). MrVBF is a topographic index which identifies domains of deposited transported material at a range of scales and is based on the observations that valley bottoms are low and flat relative to their surroundings and that large valley bottoms are flatter than smaller ones (DEM Source: Geoscience Australia 2009). Location of the study area in Australia is also shown in the inset.

Sequence A (*transported cover pre-dating deep weathering; Permo-Carboniferous)*

Overlying Archaean crystalline basement in the eastern and north-eastern Yilgarn Craton and the Albany Fraser and Paterson orogens of Western Australia are scattered remnants of Gondwanan Permo-Carboniferous fluvio-glacial transported cover that forms successions up to 150 m thick. The Permo-Carboniferous transported cover was produced by glacial erosion of the palaeohighs in the surrounding Archaean and Proterozoic basement, under a cold, arid climate (Salama & Anand 2017). The transported cover comprises boulder-rich diamictite, sandstone, siltstone and claystone filling broad or shallow valleys (Fig. 2). Transported cover in the shallow valleys in an undulating landscape is commonly proximally derived whereas, in broad valleys, it is more distally derived. Topographic variations cause significant lateral variations in thickness of the Permian succession, which pinches out toward the basement palaeohighs (Salama *et al*. 2016a; Salama & Anand 2017). Permo-Carboniferous transported cover and underlying bedrock were subjected to intensive, post-Permian chemical weathering (Eyles & de Broekert 2001; Anand & Paine 2002; Anand & Robertson 2012; Salama & Anand 2017; Salama & Anand, 2018a,b). Permian transported cover is commonly poorly indurated, strongly weathered and ferruginised (resulting in mottling, and the development of nodules and pisoliths). Some of the deeper glacial deposits and underlying bedrock are unweathered. Thus, several exploration environments can be encountered in areas dominated by Permian transported cover (Fig. 2), including fresh to highly weathered clays with or without strong ferruginisation (chemical interface) towards the top of the succession. Permian transported cover may be overlain by Sequences B and C, described below.

Sequence B (transported cover deposited contemporaneously with weathering; Mid Eocene- Miocene)

Large broad palaeovalleys representing older drainage systems are mantled with deeply weathered profiles. Both the palaeovalleys and the overlying weathered material were incised by smaller inset-valleys (‘palaeochannels’; Fig. 2). Major incision occurred in the Middle Eocene and was primarily caused by epeirogenic uplift of the Yilgarn Craton (de Broekert & Sandiford 2005). Filled inset-valleys form a large buried network in the Yilgarn Craton and may occupy up to 30% of the landscape. They are many kilometres long and up to 1-2 km wide (Anand & Paine 2002).

continued on page 10

Gold dispersion in transported cover sequences especially in… *continued from page 9*

The nature of the transported cover varies between the palaeovalleys and inset-valleys (Fig.2). In palaeovalleys, the transported cover is shallow and largely consists of colluvial-alluvial detritus, derived locally from upslope erosion that accumulated on footslopes and valley floors within a toposequence. Iron oxide cementation of detritus in palaeovalleys formed ferricrete (chemical interface; Anand *et al*. 2019). Ferricretes are generally underlain by lateritic residuum, which is formed from weathering of underlying bedrock. Overprinting of ferricretes has occurred in palaeovalleys as the transported cover was subsequently reweathered by groundwater in the presence of organic matter. Goethite and kaolinite were precipitated to form yellow cortices and authigenic pisoliths, and voids and cracks were filled. Evidence for the interaction of vegetation and microbes with ferricrete is preserved in root channels, organic carbon and microbial fossils, confirming significant biological modification (Anand *et al*. 2017, 2019).

Transported cover in inset-valleys is alluvial, lacustrine or estuarine (Kern & Commander 1993; Anand & Paine, 2002; de Broekert & Sandiford 2005). At the base of an inset-valley, transported cover is a coarse-grained (sand and gravel) fluviatile unit of Middle to Late Eocene (the Wollubar Sandstone; physical interface). This unit is unconformably overlain by a clay-rich unit of probable Oligocene-Miocene age (Perkolilli Shale; Kern & Commander 1993). Transported cover is up to 100 m thick and was derived from erosion of a pre-existing weathered profile. The inset-valley transported cover is commonly overprinted by ferruginisation and in places by silicification, calcification and dolomitisation. Ferruginisation (chemical interface) is widespread as megamottles or nodules, pisoliths or massively cemented zones at upper levels, mostly, but not exclusively, above the modern water table (Anand & Paine 2002).

Sequence C (transported cover deposited during the arid period; Quaternary)

A wide range of transported cover (colluvial, alluvial, aeolian, evaporitic) may overlie not only fresh and weathered basement, but also the older cover, and consist of their physical and chemical weathering products. This type of transported cover, a few metres to 25 m thick, is derived from the combination of increased erosion of the land surface due to tectonic uplift, and a shift to more arid conditions during the Late Miocene to Quaternary (Anand & Paine 2002). At many sites, the colluvium-alluvium is composed of two major sedimentary units: an upper yellow to red, sandy silty clay and a lower, red-brown, gravelly sandy clay. Viewed together, the sandy silty clay and gravelly, sandy clay units represent an inverted stratigraphy in relation to the residual regolith from which they were derived, in that material derived from the upper ferruginous duricrust occurs at the base of this surficial transported cover. The sandy, silty clay unit varies from 2 to 10 m thick, and overlies ferruginous duricrust, saprolite or more commonly a gravelly sandy clay unit; that is derived by erosion of saprolite and saprock. The upper parts of the transported cover have been variably silicified and calcified (chemical interface) possibly enhanced by short periods of water saturation (Anand & Paine 2002).

Quantification of weathering of transported cover

Weathering indices can provide a quantitative measure of the extent of weathering of bedrock and transported cover. Several weathering indices (e.g., Ruxton Ratio, Weathering Index of Parker, Vogt's Residual Index, Chemical Index of Alteration, Chemical Index of Weathering, Plagioclase Index of Alteration, Silica-Titania Index), have been proposed to characterise the intensity of weathering and weatherability depending upon the nature and requirement of the study (Price & Velbel, 2003). Among the weathering indices evaluated by Price & Velbel (2003), the weathering index of Parker (1970, referred to here as WIP) is the most appropriate, because it includes the highly mobile alkali and alkaline earth elements (Na, K, Mg, Ca) in its formulation

$$((100)[(2Na_20/0.35)+(MgO/0.9)+(2K_2O/0.25)+(CaO/0.7)])$$

thus yielding values that differ greatly from those of the parent rock. In addition, the WIP allows for Al mobility, unlike other weathering indices. The WIP is >100 for fresh rock whereas for highly weathered rock it is 0. Figure 5 shows the WIP for various transported cover units in three sequences from various localities in the Yilgarn Craton. Residual regolith (saprock, lower, middle and upper saprolite) is also included for comparison. As expected, the WIP of saprock (median 73) and lower saprolite (median 53) are much greater than middle (median 27) and upper saprolite (median 10). The WIP values for three sequences are less than 20 with the exception of fresh diamictite (median 97) suggesting the transported cover is highly weathered and weathering may have happened before or after deposition. Higher WIP indices in recent transported cover, compared to older transported cover reflect some minor smectite and illite formation during the arid period (Anand & Paine 2002).

continued on page 11

Gold dispersion in transported cover sequences especially in… *continued from page 10*

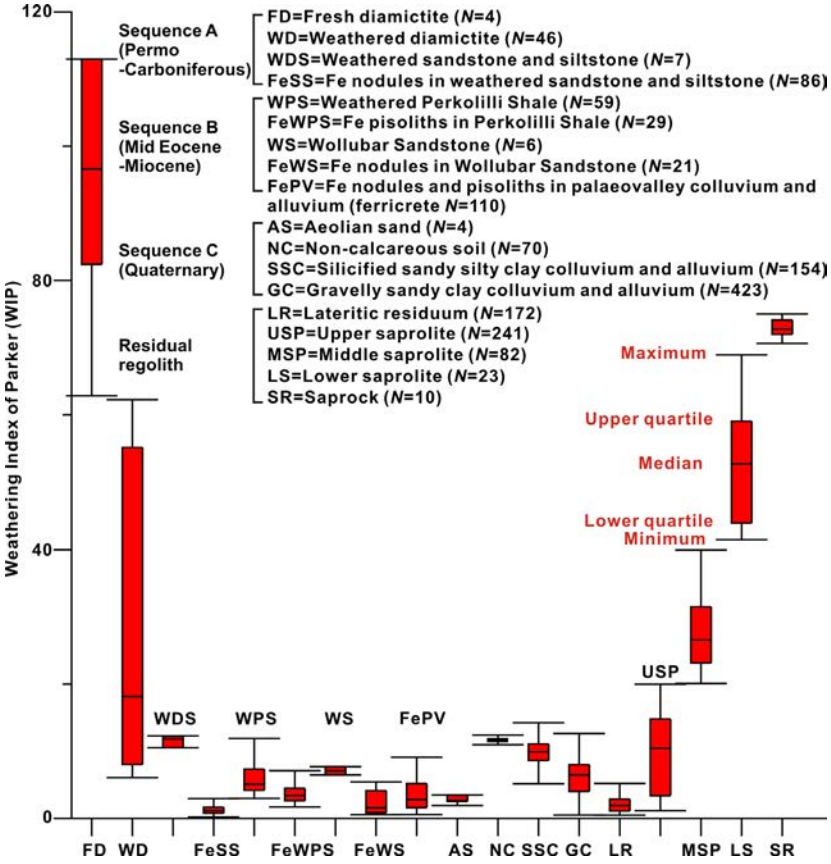

Figure 5. Comparison of Weathering Index of Parker (WIP; Parker 1970) values for transported cover collected from various regolith studies. The Parker index was calculated using the formula: (100)[(2Na_2 0/0.35)+(MgO/0.9)+(2K_2O/0.25)+(CaO/0.7)]. Upper saprolite also includes samples from the plasmic zone.

Si, Al and Fe in transported cover

Silica, Al and Fe distributions show the extent of silicification, kaolinisation and ferruginisation of transported cover (Fig. 6). Although ferruginisation can occur in any type of transported cover, older cover is generally strongly ferruginised to form nodules and pisoliths compared to recent cover that is silicified to form red-brown hardpan. Ferruginous pisoliths in the Perkolilli Shale differ from ferruginous nodules in weathered diamictites and the Wullabar Sandstone by having abundant Fe as goethite and much less Si and Al (as quartz and kaolinite). In addition to hematite and goethite, quartz is important in ferruginous nodules formed in the Wullabar Sandstone and diamictites. There is an overlap of the Perkolilli Shale with weathered diamictites but weathered diamictites are more quartz-rich. Recent gravelly colluvium and alluvium can be distinguished from silicified colluvium and alluvium by having abundant Fe (as hematite, goethite, maghemite) as detrital clasts and less Si (opaline Si and quartz). The Wollubar Sandstone and aeolian sand are Si-rich.

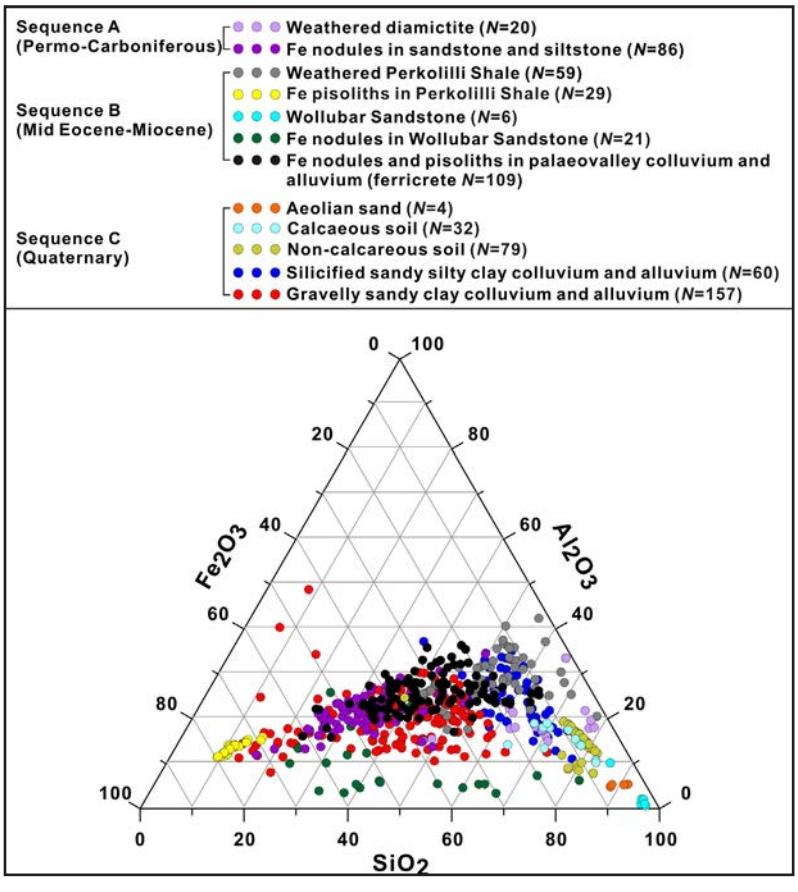

Identification of transported cover

Transported cover can be distinguished by an obvious textural and chemical discordance with the underlying residual regolith, preserved sedimentary structures and poorly ordered kaolinite (Anand & Paine 2002). The selection of elements used to identify transported cover from residual regolith should be based on their immobility in the weathering environment, so as to remain in high concentrations in a weathering profile (Hallberg 1984). Zirconium and Ti are very widely used as immobile elements, mainly because they occur in most rocks only as the minerals zircon, anatase and rutile, which are resistant to weathering. Two environments where the inset-valley and Permian

Figure. 6. Ternary diagram showing composition of various categories of transported cover in terms of Al, Si and Fe content.

continued on page 12

Gold dispersion in transported cover sequences especially in… *continued from page 11*

transported cover overlie saprolite (Fig. 7) may be compared in this way. In both cases, Ti/Zr ratios are useful for discriminating transported cover from underlying *in situ* regolith (Fig. 7). However, Ti/Zr ratios do not clearly separate the weathered diamictite from inset-valley clays and recent colluvium and alluvium. This implies that all types of transported cover in this environment are derived from a similar lithology (felsic) and are unrelated to the underlying mafic-ultramafic basement.

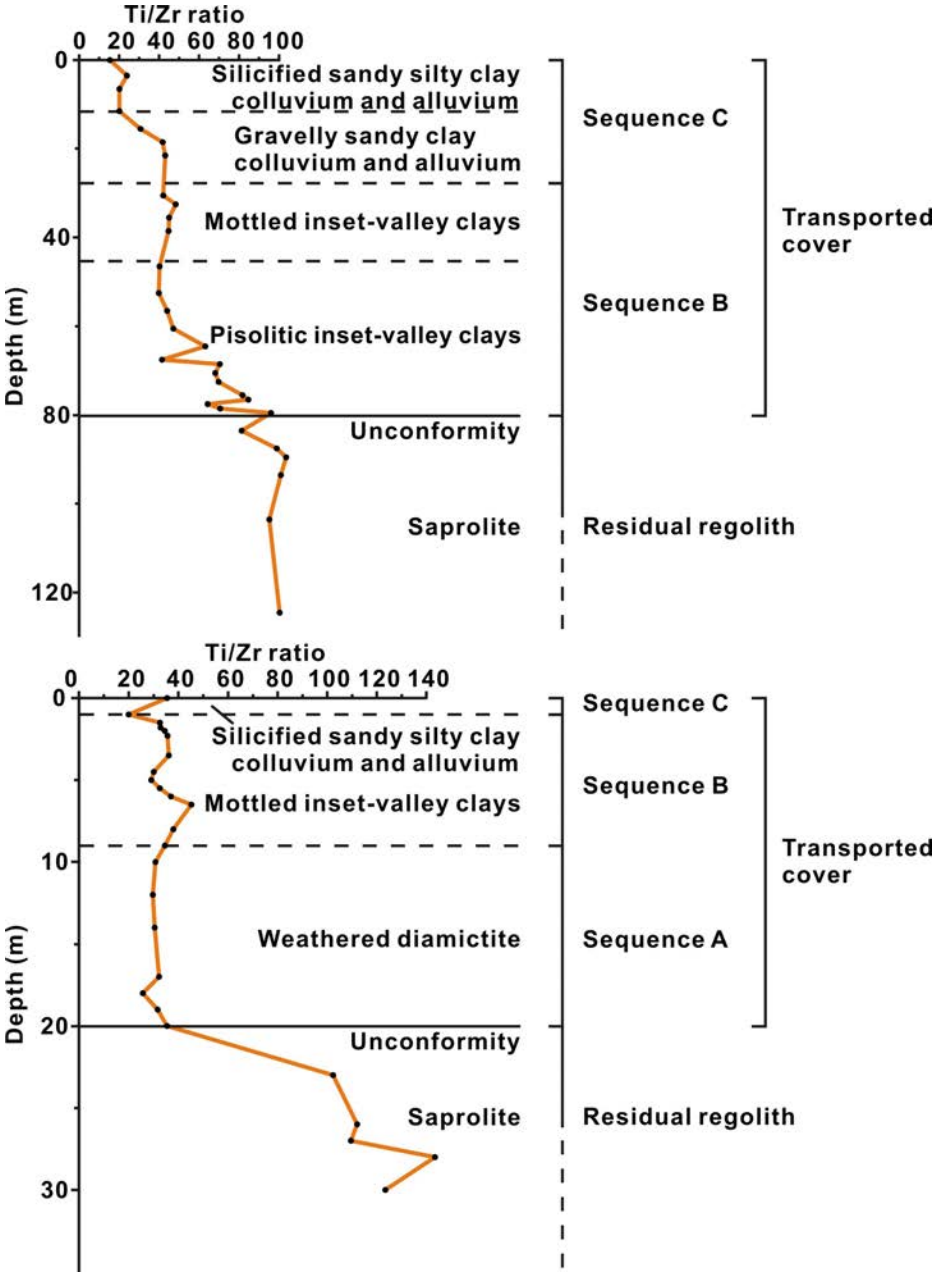

Figure 7. Ti/Zr ratios showing discrimination of transported cover from residual regolith. Two types of transported cover environments are compared.

Metal dispersion in Sequence A (transported cover pre-dating deep weathering; Permo-Carboniferous)

Examples of dispersion from gold deposits into Permian transported cover are from Toppin Hill and Smokebush (Salama & Anand, 2018a,b), Havana and Tropicana (Lintern *et al*. 2009), Calibre (Noble *et al*. 2019), Redeemer (Baker 1991; Carver *et al.* 2005), and Lancefield South (Anand & Robertson 2012). Toppin Hill and Smokebush (Yamarna Terrane), Havana and Tropicana (Albany Fraser Orogen) and Calibre (Paterson Orogen) represent the D1 environment (Figs. 2 and 4) where extensive sheets of quartz, goethite-hematite-rich authigenic ferruginous nodules and pisoliths (palaeoredox front) occur at the top of Permian transported cover that are typically overlain by recent aeolian sand, the lower part of which may also contain authigenic pisoliths and nodules. Here, the Permian transported cover is deeply weathered and consists mainly of coarse-grained gravelly, kaolinitic and micaceous (illite and muscovite-rich) saprolitic sandstones and siltstones at the base, grading upwards into mottled, cross-laminated sandstones and siltstones with a variety of dissolution features such as dissolution-collapse brecciation. This type of transported cover is markedly different from Permian glacial diamictites (e.g., Redeemer, Lancefield South) in the northeast part of the Yilgarn Craton (Anand & Robertson 2012; Salama *et al*. 2016a; Salama & Anand 2017). At the Redeemer and Lancefield South gold deposits, authigenic nodules and pisoliths are not developed but the transported cover is mottled near the top. Redeemer provides an example of mechanical dispersion of mineralised detritus into Permian transported cover (environment D2; Fig. 2) whereas the Lancefield gold deposit provides an example of initial mechanical to residual dispersion followed by hydromorphic dispersion at the palaeoredox front (environment D3; Fig. 2).

Toppin Hill, Smokebush, Havana, Tropicana and Calibre gold deposits (environment D1)

The Yamarna greenstone belt (Smokebush, Toppin Hill) is dominated by metamorphosed mafic rocks, with less common ultramafic, felsic metavolcanic and volcanoclastic rocks, clastic metasedimentary rocks and chert units (Bath *et al*. 2016). The Toppin Hill mineralised lode, which is only 5-10 m wide, contains Au (3-21 ppm), Cu (210-500 ppm), S (7150 ppm-1.26 %), Zn (<100 ppm) and Pb (<20 ppm). The Permian transported cover at this prospect is up to 45 m thick

continued on page 13

Gold dispersion in transported cover sequences especially in… *continued from page 12*

(Salama & Anand 2018a,b). Here, authigenic pisoliths developed in Permian transported cover are overlain by up to 6 m of aeolian sand. The residual weathering profile is mainly bleached kaolinitic saprolite over granitoids, and ferruginous saprolite over felsic volcanics and metabasalt. Gold in the Permian transported cover sequence varies between 10 and 100 ppb and is in high concentrations in the upper mottled sandstones and the basal gravelly sandstones and conglomerates, compared to concentrations in siltstone intercalations. Forty eight samples of authigenic nodules and pisoliths were collected for analysis from near the surface (10-30 cm). Results for Au from two traverses from Toppin Hill (Fig. 8) show that Au in authigenic pisoliths clearly reflects the buried mineralisation. In traverse 1, Au reaches 30 ppb over the mineralisation compared to a background of less than 10 ppb (Fig. 8A). Similarly, strong Au anomalies (Au 52-605 ppb) were identified in traverse 2 over the mineralisation (Fig. 8B). This indicates that gold has been dispersed chemically from the mineralisation through the Permian cover to the authigenic pisoliths above. During Palaeocene-Miocene wet climatic events, the water table could have been near the surface with metals dispersing from buried weathered ore to the top of the water table. This may have led to mobilisation and precipitation of metals from the residual weathering profile through the Permian transported cover. The area in general is strongly faulted and fractured but the extent of faulting in Permian cover is unknown. Therefore, the role of geochemical dispersion through fractures at Toppin Hill is unclear.

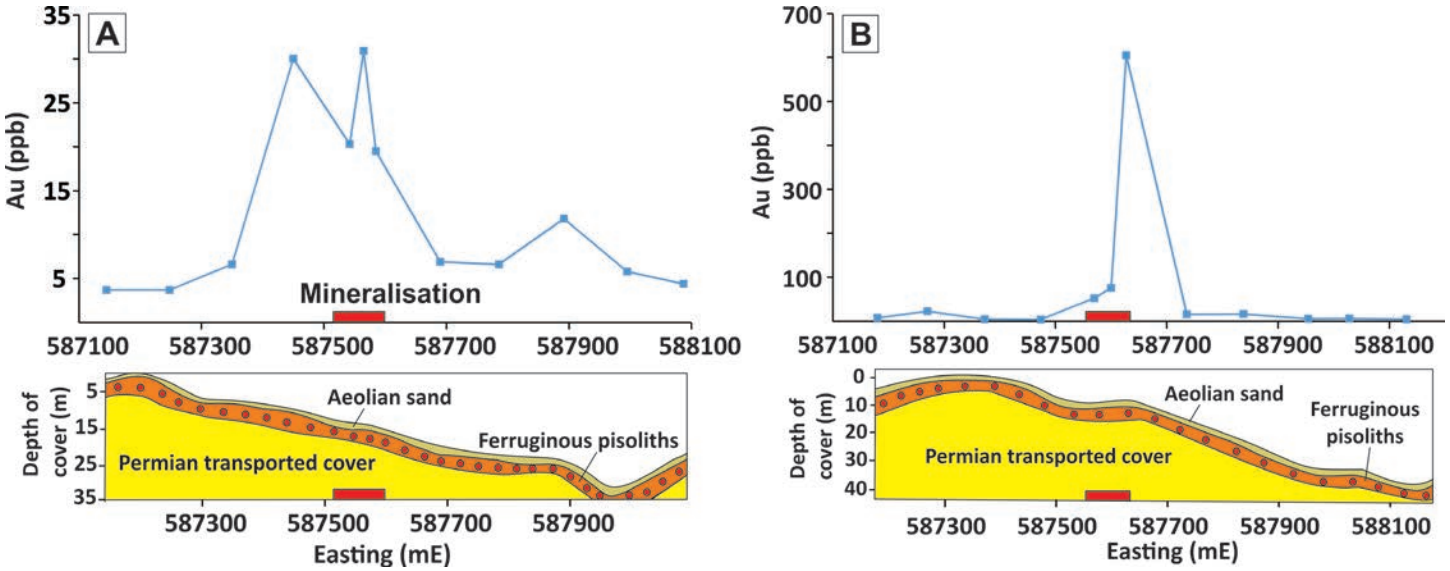

Figure 8. (A,B) Regolith cross sections showing variation in transported cover for two traverses, Toppin Hill gold prospect. Elevated gold contents in authigenic ferruginous pisoliths (red dots in orange unit) developed at the top of Permian cover indicates the location of mineralisation.

At Smokebush, mineralisation occurs within a 25 m wide shear zone in quartz-rich metadolerite, over a 800 m long strike length with localised quartz and sulphide lode structures (Bath *et al*. 2016). The ore zone contains Au (11 ppm), As (7.10 %) and S (3.58 %). The Permian transported cover is 5-30 m thick and rest unconformably on a 25-60 m thick saprolite developed over sheared dolerite (Salama & Anand 2018a,b). The unconformity between the Permian transported cover and the underlying saprolite is marked by a basal gravelly layer of rounded, quartz-rich clasts. There are two types of ferruginous materials at the 2-10 m thick palaeoredox front at the top of the Permian transported cover. These are, (i) quartz-hematite-goethite-rich authigenic nodules and pisoliths (<20 mm diameter) in recent quartz-rich aeolian sand and (ii) hematite-gibbsite-rich reworked ferruginous gravel formed from weathering of underlying rock. One hundred and twelve samples of ferruginous nodules and pisoliths were collected from shallow (<10 m) drilling and the near surface (Salama & Anand 2018b). The authigenic ferruginous nodules and pisoliths have anomalous Au and As concentrations over bedrock mineralisation (Salama & Anand 2018a). Gold varies from 1 to 135 ppb with the majority of samples >11 ppb over mineralisation against a background of <4 ppb. Gold concentrations in authigenic pisoliths and nodules are greater than most of the underlying reworked ferruginous gravel, except in three drill holes, where Au reaches 384 ppb in reworked gravel. Conversely, the As content is greater in the reworked gravel than in the authigenic nodules and pisoliths, except for one drill hole where As reaches 2880 ppm in the authigenic pisoliths. The Permian transported cover underneath these materials is barren with respect to Au, except at the interface between the saprolite or bedrock and the Permian cover. It is concluded that the formation of anomalies in the authigenic ferruginous nodules and pisoliths indicates active hydromorphic dispersion and bioturbation through cover, whereas displaced ferruginous gravel anomalies highlight the role of the mechanical processes along slope. Thus, understanding palaeolandscape evolution and the metal dispersion mechanisms is critical for interpreting the formation of surface and interface anomalies.

continued on page 14

Gold dispersion in transported cover sequences especially in… *continued from page 13*

The Tropicana-Havana gold deposit is hosted within Neoarchaean gneisses of the Plumridge Terrane that occurs along the eastern margin of the Archaean Yilgarn Craton in the Albany Fraser Orogen. Mineralisation is located in a metasyenite of the Tropicana Gneiss (Doyle *et al*. 2017). Sulphides within the ore zones are dominated by fine pyrite (2-8%, <0.2mm) and minor chalcopyrite, electrum and tellurides. Although lacking significant supergene enrichment, the dominance of mineralised basement-derived clasts in the upper part of the transported cover were ore-grade and contributed mineable material at Havana (Doyle *et al*. 2017). Open pit operations at Tropicana are distributed along a northeast trending mineralised corridor 1-2 km wide and 5 km long. Along this trend, the ore deposit is partitioned by east to east-southeast shears into four principal zones from north to south; Boston Shaker, Tropicana, Havana and Havana South (Doyle *et al*. 2017).

At Tropicana-Havana, both basement and transported cover have undergone weathering to 40-50 m since emplacement (Lintern *et al*. 2009). Saprolite is unconformably overlain by 10-20 m thick Permian transported cover that are in turn overlain by recent 2-10 m thick aeolian sand (Fig. 9A) similar to the Smokebush and Toppin Hill gold deposits. On higher ground, particularly at Havana, ferricrete is 2-3 m thick and consists largely of authigenic goethite- and quartz-rich ferruginous nodules and pisoliths and a few detrital hematite-rich pisoliths (Fig. 9B). Where ferricrete has been eroded, it forms a dispersion train down slope. The accumulation of Fe to form cemented nodules and pisoliths (ferricrete) on the rise upslope to the Havana deposit is thought to reflect topographic inversion (Lintern *et al*. 2009). Ferruginous nodules and pisoliths were collected where available from drill cuttings, small pits and from the surface. At Havana, surficial nodules and pisoliths were absent above mineralisation and therefore could not be analysed but samples upslope of the projected mineralisation were strongly anomalous (550 ppb Au) (Fig. 9C; Lintern *et al*. 2009). Laser ablation ICP-MS analysis of ferruginous nodules and pisoliths shows that Au and Cu are controlled by goethite that mainly occurs in the cortex of pisoliths (Fig. 9D). At Tropicana (not shown), anomalous concentrations of Au (up to 18 ppb) occur over the mineralisation.

The Calibre Au-Cu-Ag-W deposit is located in the Paterson Orogen of Western Australia. The geology of the Calibre deposit is Proterozoic, with predominantly sulphide bearing metasediment hosted hydrothermal shear, fault and strata/

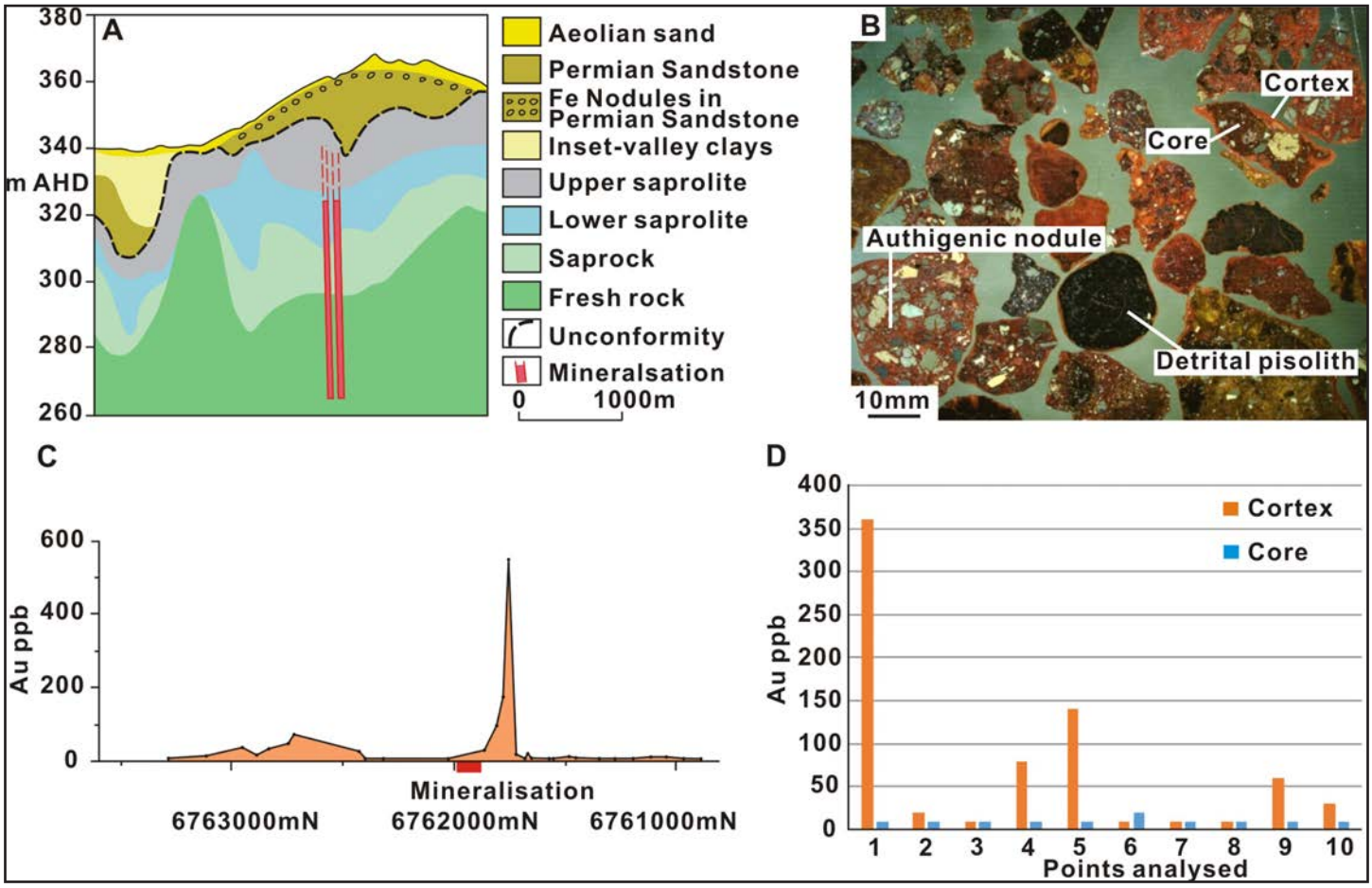

Figure 9. (A) Regolith cross section for the Havana gold deposit (modified after Anon, 2009). (B) photograph of ferruginous nodules and pisoliths showing the internal structure of authigenic and detrital pisoliths. (C) Gold content in the whole samples of ferruginous nodules and pisoliths developed at the top of Permian cover locates the mineralisation (modified after Lintern et al. 2009). (D) Laser ablation ICP-MS analysis of cores and cortices showing Au is more enriched in the cortices than the cores.

continued on page 15

Gold dispersion in transported cover sequences especially in… *continued from page 14*

contact controlled precious and/or base metal mineralisation. The mineralisation is thought to be granite related (Antipa Minerals, media release, January 2018). The deposit lies beneath 70 to 85 m of weakly consolidated and lithified Permian transported cover. The upper part of the Permian transported cover has been ferruginised to form a 5-10 m thick layer consisting of Fe nodules that are overlain by 5-15 m of recent aeolian sand. Samples from the interface between weathered and/or fresh rock and the overlying Permian transported cover and the interface between the ferruginous nodules at the top of Permian cover were analysed (Noble *et al.* 2019). At both locations, samples have anomalous concentrations of Au, Ag, Cu, As, Bi and W. Though there are much greater concentrations of W (up to 570 ppm) and Bi (up to 2.6 ppm) at the basement-transported cover interface, As and Ag are more abundant in the palaeoredox front (ferruginous nodules). Dispersion at the interface is largely mechanical, that at the palaeoredox front is chemical.

Redeemer and Lancefield South gold deposits (environments D2 and D3)

Redeemer

The Redeemer gold deposit lies within the western limb of the Lawlers antiform, in the northern part of the Norseman-Wiluna belt of the Yilgarn Craton (Fig. 4). From east to west, the stratigraphy of the western limb of the antiform consists of greenstone (layered gabbro, basalt and komatiites), overlain by metasedimentary rocks of the Scotty Creek Formation. The stratabound mineralisation is in a thick mafic metaconglomerate unit near the base of the Scotty Formation (Baker 1991). Permian transported cover is up to 25 m thick, consisting of rounded weathered granite boulders at the base, overlain by kaolinitic clays. A 5 m thick inset-valley overlying Permian transported cover contains a mixture of cobbles, ferruginous nodules, quartz and fresh mafic rocks clasts (Baker 1991).

Transported cover is underlain by residual regolith formed on basement. The depth of weathering of basement is about 50 m over the ultramafic rocks and about 25 m over the mafic metaconglomerates. Permian transported cover was investigated on a sampling grid of 10 x 2 m by combining drilling and pit wall samples (Baker 1991). There is a close correlation between Au and Bi distributions in the fresh rock and residual regolith over the mineralisation in the mafic metaconglomerate. Gold and Bi distributions show the same relationship in the Permian transported cover adjacent to the ore-bearing mafic metaconglomerate where the ore has been mechanically incorporated into the cover (Carver *et al*. 2005). In the near surface, the mafic metaconglomerate is depleted in Au relative to Bi. The relationship is similar for the Eocene-Miocene transported cover in the base of the inset-valley. Gold is dispersed from the weathered mafic conglomerates into the inset-valley cover. This dispersion is not associated with any obvious weathering in the transported cover and is likely to be mechanical (Carver *et al.* 2005).

Lancefield South

At Lancefield South, a 25 m thick deeply weathered ferruginised Permian fluvial sequence is exposed unconformably overlying weathered metamorphic Archaean rocks (Anand & Robertson 2012). The depth of weathering of the Archaean basement exceeds 50 m and is represented by well-developed kaolinitic and ferruginous saprolite. The bedrock consists of metakomatiites, metamorphosed Mg basalts, massive to pillowed mafic metavolcanics, carbonaceous shale and chert (Hronsky *et al.* 1990). The orebody consists of a mineralised zone some 140 m long and 7-12 m wide, enveloping a 5m wide lens of chert. The chert has a sulphide (pyrrhotite-pyrite-sphalerite-chalcopyrite-arsenopyrite) content of around 15% near the ore zone. Near the chert, the regolith developed on metamorphosed ultramafic rocks also contains significant supergene gold mineralisation (Hronsky *et al.* 1990).

The basal Permian is a coarse, matrix-supported conglomerate, consisting of a variety of rounded and angular metavolcanic, granitic and BIF cobbles and boulders, set in a gritty matrix of similar composition, interbedded with gritty, cross-bedded sandstones (Anand & Robertson 2012). The lower part is weathered to kaolinite, whereas the upper part is mottled. An inset-valley clay unit, 3-8 m thick, overlies the mottled Permian transported cover. Saprolite contains anomalous contents of Au and As. The Permian transported cover is enriched in Au (to 120 ppb), As (to 550 ppm) and Cu (to 150 ppm), with two distinct horizons enriched in Au. One is at the clay-rich base, and the other near the mottled top of the unit (Anand & Robertson 2012). The whole Permian transported cover sequence is anomalous in As, especially the middle to upper part. The Cu distribution is similar to that of As. Electron microprobe analysis of mineral phases showed that hematite and goethite are the main carriers of As (mean 1260 ppm) and Cu (mean 295 ppm) in mottled Permian cover. Basal inset-valley transported cover is also weakly anomalous.

Anomalies in ferruginised Permian cover were formed by residual to mechanical dispersion followed by post-depositional hydromorphic dispersion in later formed Fe oxides of mottles. Permian cover was deposited on residual soil, largely derived from mechanical breakdown of the basement containing some mineralised material, followed by limited weathering and pedogenesis. This formed anomalous concentrations of Au, Cu, Zn and As at the base of the Permian cover. However, strong dispersion (e.g., Au and As) not only occurred at the base but also at other levels, especially near the top of the Permian, largely associated with mottling which appears to represent a palaeoredox front or fronts associated with old water tables (Anand & Paine 2002).

continued on page 16

Gold dispersion in transported cover sequences especially in… *continued from page 15*

Metal dispersion in Sequence B (transported cover deposited contemporaneously with weathering; Mid-Eocene to Miocene)

Moolart Well gold deposit (environment D4)

There are two types of situations envisaged in this sequence as discussed above. These include (i) transported cover in a palaeovalley and (ii) transported cover in an inset-valley (Fig. 2). In the palaeovalley environment, the transported cover is strongly ferruginised to ferricrete (chemical interface) that is generally underlain by lateritic residuum. Ferricrete is nodular to pisolitic and occurs along the flanks of the inset-valley. Because of lateral dispersion in the palaeovalley, geochemical anomalies are large, measuring hundreds of metres to several kilometres in length for Au and pathfinder elements in pisoliths and nodules (e.g., Moolart Well, Mt Gibson, Bulchina, Empire and Gourdis gold deposits; Anand *et al*. 2019). However, ferruginous nodules and pisoliths may contain ore-grade gold with or without any known significant underlying primary mineralisation. Moolart Well (Fig. 4) typifies this environment where the ferricrete deposit extends over 4 km north-south and up to 1 km east-west (Fig. 10), and has an average thickness of 4 m (Balkau *et al*. 2017). The local

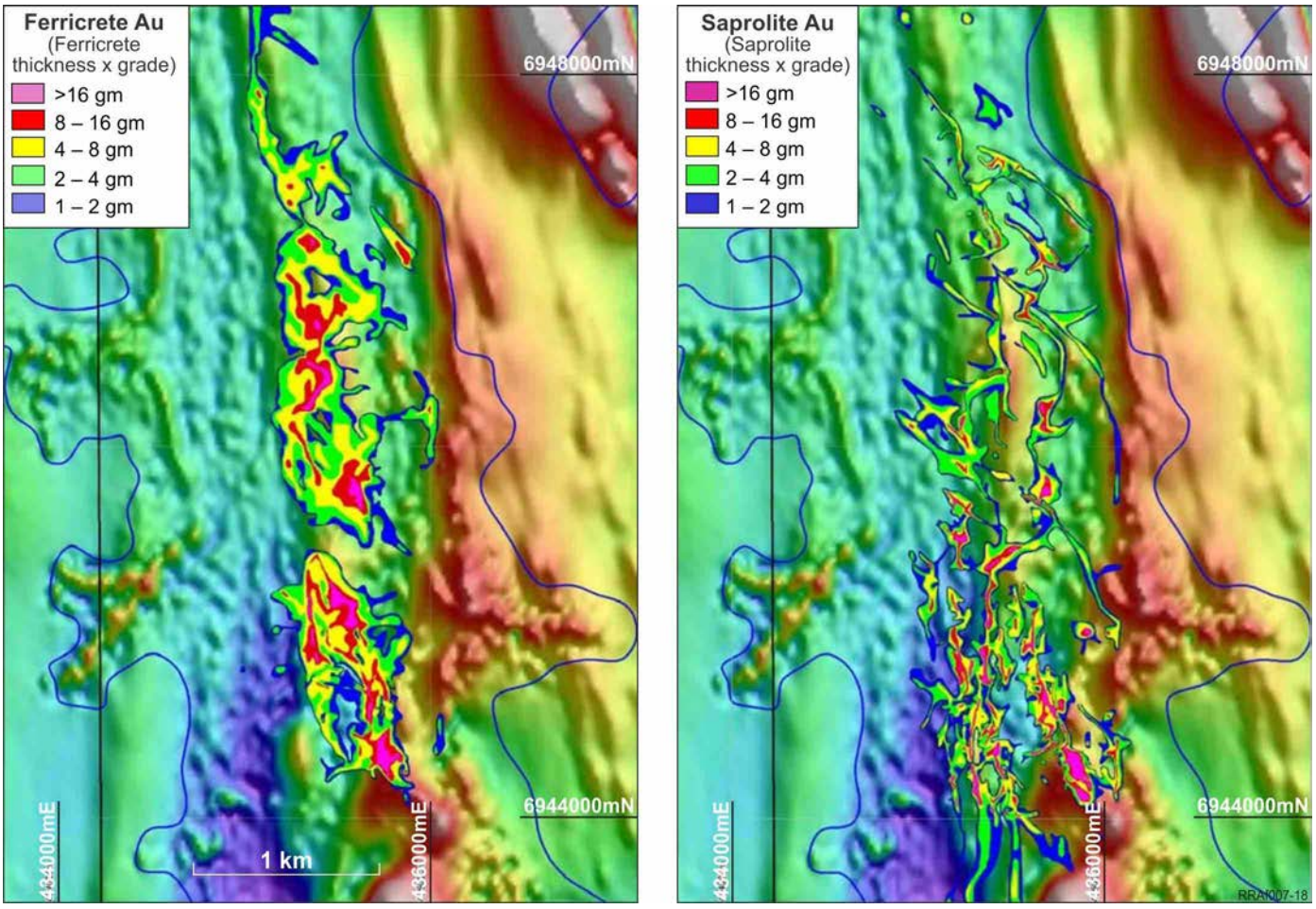

Figure 10. Gold concentrations in ferricrete and saprolite gold deposits, Moolart Well. Outline of inset-valley defined by magnetic imagery is also shown (blue line) (modified after Anand et al. 2017).

Archaean stratigraphy is a sequence of high Mg metabasalt with interbedded chert and sulphidic metasedimentary rocks (Balkau *et al*. 2017). The low-grade primary mineralisation (0.3–0.5 g/t Au; 103,000 ounces Au) beneath the ferricrete gold deposit is hosted predominantly in intermediate metadiorite intrusives within a north-trending shear zone. The principal economic deposits are secondary and confined to (1) an upper, flat-lying layer of goethite-coated ferruginous pisoliths formed in palaeovalley cover (1.19 g/t Au; 525,000 ounces Au); and (2) an underlying Au-bearing saprolite (0.75 g/t Au; 1,096,000 ounces Au), derived from weathering of the primary mineralisation (Balkau et al. 2017). The ferricrete gold deposit is overlain by younger silicified colluvium and alluvium (red-brown hardpan) which is 1–3 m thick on the east side and increases to >10 m along the western side of the ferricrete gold deposit.

Four hundred and seven samples of ferricrete, silicified colluvium and alluvium, soil and weathered bedrock, each approximately 1 kg, were collected and analysed from eight profiles at 0.25 m vertical intervals to depths of 12-15 m through the deposit (Anand *et al*. 2017). The highest concentrations of Au (to 10360 ppb) in ferricrete are similar to the concentration in the mineralised saprolite (to 9030 ppb) but high concentrations (to 6650 ppb) also occur over

continued on page 17

Gold dispersion in transported cover sequences especially in… *continued from page 16*

unmineralised saprolite, where the overall concentration relative to the saprolite is over x10 or more. In contrast, there are significant As concentrations (>500 ppm) in ferricrete over mineralised saprolite, but are greatly reduced (50–100 ppm) distant from mineralised saprolite. Furthermore, the data demonstrate a preferential enrichment of Au in pisoliths with goethite-coated cortices (Anand *et al*. 2017). Gold characteristically shows an increase in grade and purity (no Ag) in ferricrete compared to the underlying saprolite. Gold in nodules and pisoliths is mostly secondary (Ag-poor) nanometre- to micron-sized spheres, irregular, chains, hexagons, triangles and wires in precipitates of organic C, goethite, kaolinite and amorphous Si within cortices, cracks and cavities in pisoliths (Fig. 11). Secondary Au occurs as clumps and large clusters in organic C-rich zones of the cortices and cavities of pisoliths, implying a role for organic processes in their formation (Anand *et al*. 2017).

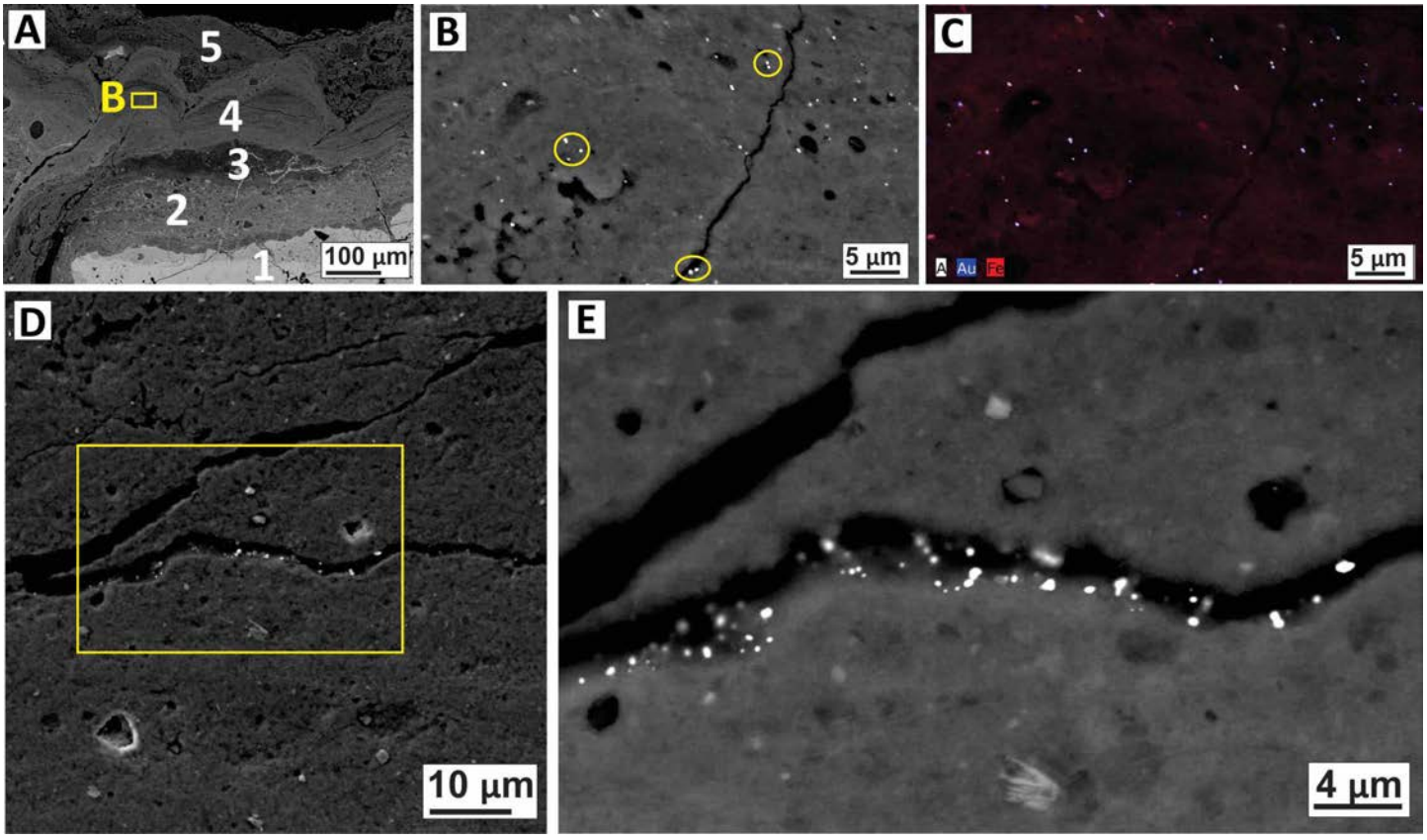

Figure 11. (A) SEM images of a sectioned pisolith from ferricrete showing hematite-rich core (1), goethite cortex (2), kaolinite cortex (3), goethite cortex (4) and goethite-kaolinite cortex (5), Mt Gibson. Boxed area in A is shown in B. (B) Multiple Au grains in goethite cortex and cavities. Some Au grains are highlighted by yellow circle. (C) Element map (EDX) of Au and Fe content of the same box shown in B. (D) Au grains in cavities of core. Boxed area in D is shown in E. (E) High magnification image of Au grains in cavity (after Anand et al. 2019).

Gold in ferricrete is sourced from mineralisation; proximally (from underlying saprolite), distally (from updrainage or from flanking valleys), or from all of these (Anand *et al*. 2017, 2019). Evolution of ferricrete gold deposits has involved several stages of mechanical, biological and chemical mobilisation and reprecipitation of Au into a palaeovalley, resulting in both high concentration of Au and large dispersion haloes. Ferricretes require significant subterranean lateral influx and migration of groundwater to transport dissolved Fe and Au along and above an unconformity, during an extended period of biological and chemical weathering. This model contrasts with the comparatively simple Au and Fe enrichment of lateritic residuum as the landscape was progressively deflated by lateritic weathering.

Garden Well and Rose Dam gold deposits (environment D5)

Garden Well and Rose Dam gold deposits provide examples of the inset-valley environment (environment D5; Figs. 2 and 4). Garden Well is a shear-hosted Archaean orogenic gold deposit. Gold mineralisation occurs as oxide ore down to 70 m below the base of the inset-valley and the hypogene ore extends to a depth of 400 m (Balkau *et al*. 2017). Primary Au mineralisation consists of a 100 m wide east dipping zone in the shear zone cutting mixed metamorphosed ultramafic rocks and metasediments extending into the eastern black shale metasediments (Balkau *et al.* 2017). Lead, Zn and Cu sulphides occur within the ore. Anomalous Au values are common in the bottom 15 m of transported cover of the inset-valley.

continued on page 18

Gold dispersion in transported cover sequences especially in… *continued from page 17*

The deposit is overlain by an inset-valley (~600 m wide that runs in a north-south direction) and is concealed by up to 35 m of transported cover (Lintern *et al*. 2013b). Above the basement derived saprolite, the base of the inset-valley transported cover sequence consists of 2-4 m of ferruginous and silicified sandstone nodules, with medium grained, angular quartz grains (the Wollubar Sandstone; physical interface; Fig. 12B,C). The nodules lack or have thin (0.5 mm) goethite coatings. A 15-20 m thick sequence of kaolinitic clays (the Perkolilli Shale) overlies the sandstone (Fig. 12C). This unit contains pisoliths (chemical interface; Fig. 12A) that commonly form <10% to 20% of the lower to middle part of the clay unit. Goethite-rich cortices form the bulk of these pisoliths. Above the pisolitic clays lies 4-6 m of megamottled kaolinitic clays. Finally, the sequence is overlain by dark red-brown ferruginous gravels and nodular red clay and calcareous to siliceous colluvium and alluvium and red brown sandy soil containing abundant polymictic clasts (Lintern *et al*. 2013b).

Both the ferruginous pisoliths and the nodules are rich in Cr, V, Co, Ni and Ti from the underlying ultramafic lithology. Laser ablation ICP-MS mapping showed that Cr (Fig. 13A), V and Ti are largely concentrated in the cores of the pisoliths with some in laminations, whereas in nodules they are uniformly distributed or occur in cracks and veins (Fig. 13E). Bulk sampling of the pisoliths show multi-element anomalies in Au (Fig. 12D; maximum 805 ppb), In (Fig. 12E; maximum 0.20 ppm), Ag (maximum 0.15 ppm), As (maximum 1340 ppm), Bi (maximum 2.9 ppm), Cu (maximum 381 ppm), Pb (maximum 162 ppm), S (maximum 1310 ppm) and Se (maximum 4.66 ppm) over mineralisation (Lintern *et al*. 2013b). These elements have significant anomaly/background contrasts, in particular for Bi, In, S and Se. Zinc (maximum 504 ppm)

continued on page 19

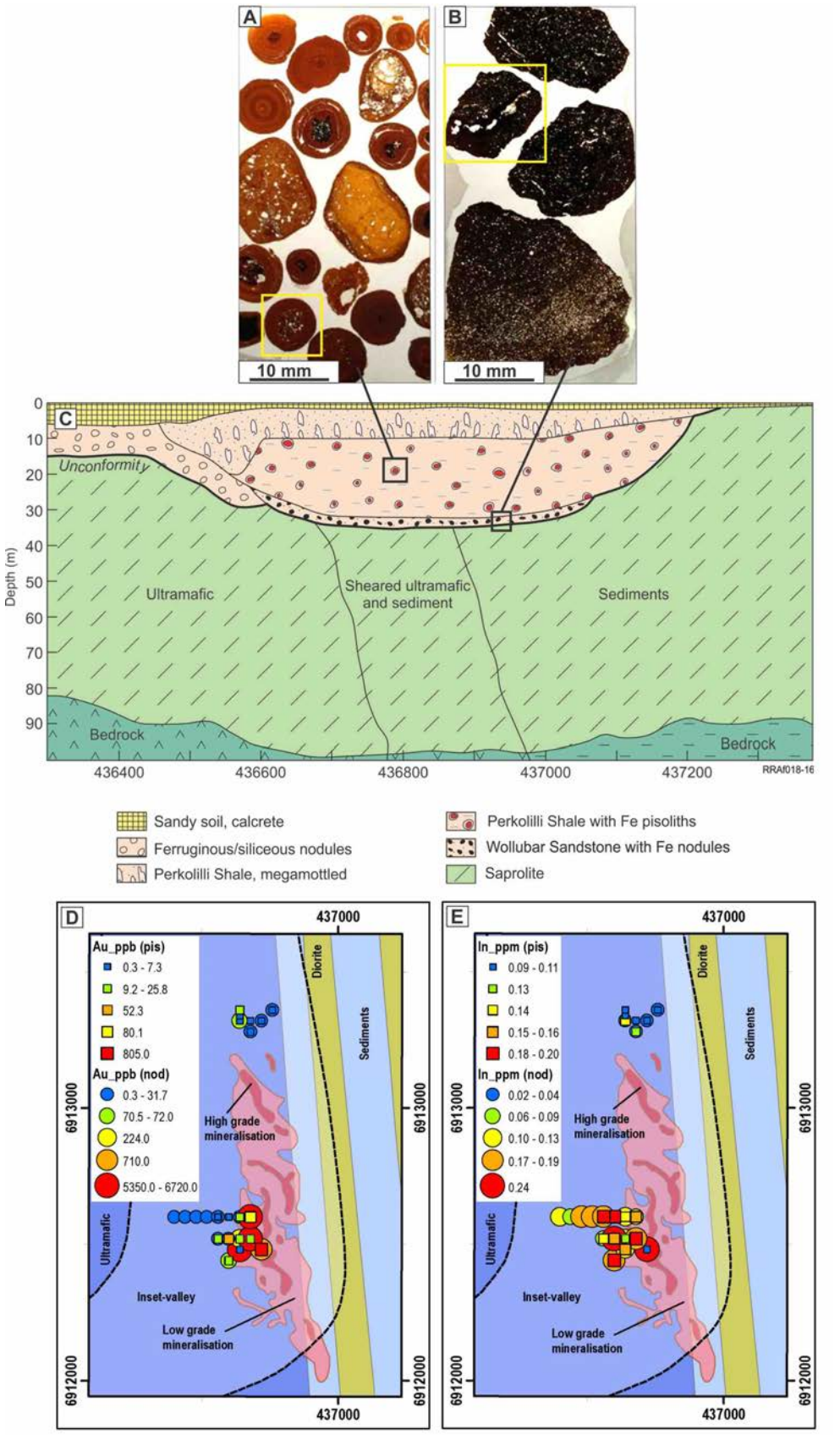

Figure 12. Photographs of (A) ferruginous pisoliths formed in inset-valley clay sequence and (B) ferruginous nodules formed at interface, Garden Well gold deposit. (C) Regolith cross section showing the stratigraphy of inset-valley transported cover. (D) Gold and In concentrations in ferruginous nodules and pisoliths relative to the location of the buried mineralisation (modified after Lintern et al. 2013b).

Gold dispersion in transported cover sequences especially in… *continued from page 18*

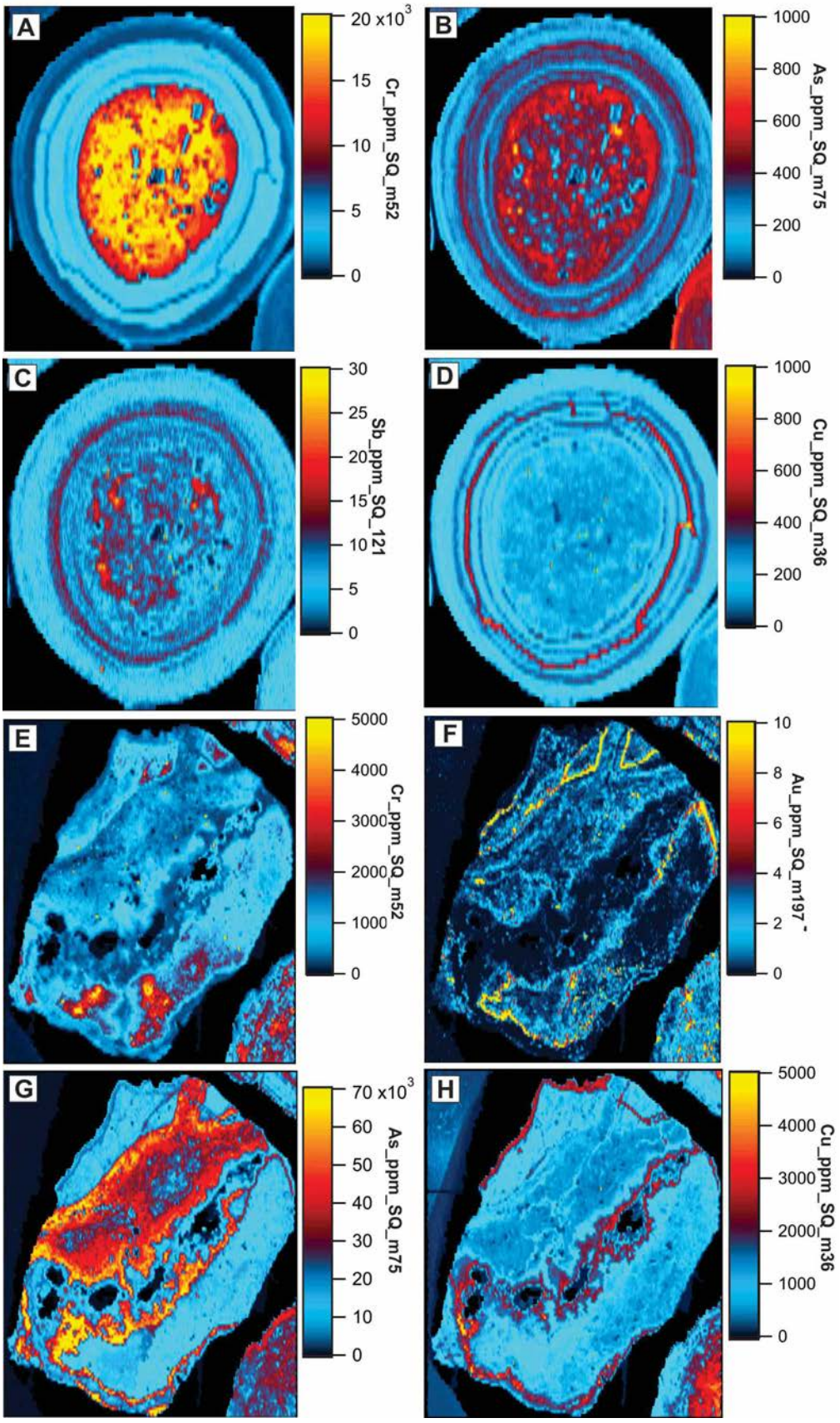

Figure 13A-D. Laser ablation ICP-MS elemental maps of a ferruginous pisolith (approximately 5 mm in diameter) shown in a yellow box in Fig. 12A; and Figure 13E-H a ferruginous nodule (approximately 10 mm in diameter) shown in a yellow box in Fig. 12B.

and Cd (maximum 0.27 ppm) are anomalous and broadly dispersed but the contrast between mineralisation and background is poor. Laser ablation ICP-MS mapping of pisoliths showed As, Cu and Sb not only occur in the core but also in laminations especially inner ones (Fig. 13B-D). Similar results were noted at the Rose Dam Gold Deposit where Cu is concentrated in cortices.

There are multi-element anomalies in nodules at the base of the inset-valley (Au (maximum 6720 ppb; Fig. 12D), In (maximum 0.24 ppm; Fig. 12E), As (maximum 5480 ppm), Bi (maximum 2.1 ppm), Cu (maximum 1741 ppm), Mo (maximum 3.6 ppm), Pb (maximum 88 ppm), S (maximum 1030 ppm), Sb (maximum 8 ppm) and Se (maximum 15. 7 ppm)). The abundances of these elements in the nodules are much greater than in the pisoliths. Visible gold was only seen in ferruginous nodules but not in pisoliths. All visible Au is micro-particulate (sizes range from 0.1 to 0.3 µm) and is confined to cavities in nodules. Authigenic Au typically contains no Ag and is secondary. Laser ablation ICP-MS mapping showed Au, As and Cu largely occur in veins and cracks (Fig. 13F-H).

There are several stages of dispersion of metals in ferruginous nodules and pisoliths of inset-valley sequence. At physical interface (the Wollubar Sandstone) there would have been physical mixing of sand with underlying anomalous weathered basement clasts that were subsequently ferruginised to quartz-goethite-hematite-rich nodules. Much of the Au in the ferruginous nodules was physically emplaced here from erosion of saprolite, followed by short-distance chemical dispersion into goethite and hematite. Strong multi-element

continued on page 20

Gold dispersion in transported cover sequences especially in… *continued from page 19*

anomalies in the Perkolilli Shale-hosted pisoliths occur in two modes, as detrital metal-rich, weathered mineralized fragments in cores or hydromorphically dispersed in goethite-rich cortical laminae. This suggests that the components of *in situ* mineralised regolith have migrated upwards into transported cover by continual redistribution during slow deposition of the clay unit. Given that the clay was most likely bioturbated during deposition, it would appear that there has been continuous interaction between the clay unit and the underlying *in situ* regolith. Bioturbation appears to be a dominant mechanism in agitating of the transported cover – an inset-valley would have supported abundant vegetation and burrowing animals.

Metal dispersion in Sequence C (transported cover deposited during arid period; Quaternary)
Calista, Bronzewing, Lawlers and Bulchina gold deposits (environment D4)

At Calista, primary mineralisation is sulphide-rich and is hosted in an overturned, steep, westerly dipping sequence of rocks. It is characterised by an association of Au, Bi, Se, Cu, Zn, Sn, W, As and Ag. At Bronzewing, gold mineralisation is associated with veins and dense stockworks of quartz within variably sheared and altered pillow metabasalts and is accompanied by pyrite, pyrrhotite, minor chalcopyrite, scheelite and visible gold. The Lawlers (North deposit) deposit lies within the Agnew supracrustal belt. Primary mineralisation occurs in quartz veins and shear zones. The Bulchina deposit is associated with quartz veining and quartz reefs. At all these sites, significant dispersion of gold and associated elements occurred into basal gravelly colluvium where it is underlain by lateritic residuum and/or ferricrete (environment D4; Figs. 2 and 4; Anand *et al*. 1989; Anand *et al*. 1993; Anand & Williamson 2000; Anand *et al*. 2001; Anand 2015). Transported cover is recent colluvium and alluvium which is about 15-20 m thick. Figure 14 shows an example from the Calista gold deposit where the dispersion of Au, Cu and As (not shown) extends from lateritic residuum to the basal gravelly colluvium and alluvium with no dispersion into soil. Examination of the size fractions of the transported cover indicates that Au is concentrated in the >2 mm fraction and is less common in the <75 m fraction, relative to the bulk sample. Hydromorphically dispersed Au would be expected to be precipitated on chemically active surfaces of Fe oxides and clays, whereas mechanical dispersion of Au would be expected to occur in ferruginous nodules and ferruginous saprolite clasts. Thus, concentration in the fine fraction would suggest mainly hydromorphic dispersion; concentration in the coarse fraction implies mechanical dispersion. Manganese nodules formed at the residual and transported cover interface show high concentrations of Cu (400-900 ppm) and Zn (200-600 ppm) but are very poor in Au (<5 ppb).

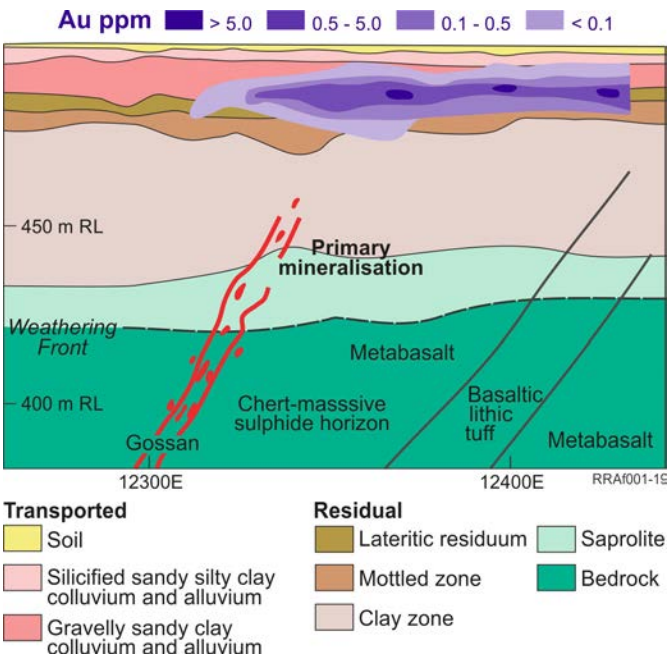

Figure 14. Cross section of the Calista gold deposit showing the regolith stratigraphy and gold anomaly (purple polygons). RL refers to the elevation above mean sea level.

Where the shallow cover (<5 m) overlies lateritic residuum or ferricrete, the whole transported cover column (except soil) can be anomalous (e.g., Moolart Well; Mt Gibson). At the Moolart Well gold deposit, the ferricrete is overlain by a widespread, silicified colluvium-alluvium (red-brown hardpan). The hardpan sampled at 1–1.5 m depth is anomalous in Au (2–350 ppb) and shows a broad halo over the ferricrete gold deposit although slightly displaced to the east. There is less Au in the hardpan than in the ferricrete, but Au is slightly enriched toward the base of the hardpan due to mixing (by bioturbation) with the upper ferricrete. This suggests that Au in the hardpan is sourced from ferricrete (Anand *et al*. 2017). Gold largely occurs as nanoparticulate spheres in the fine mass of authigenic amorphous (opaline) silica. Nanoparticulate Au spheres in amorphous Si are thought to have been deposited during a drying event after flooding (Anand *et al*. 2017).

In summary, where the transported cover is thin, bioturbation of the transported cover brings a strong anomaly close to the surface. As the transported cover thickens, bioturbation of its upper part is progressively diluted by incoming distal material until no significant anomaly remains.

Quasar, Harmony and Gruyere gold deposits (environment D6)

Gold mineralisation at Quasar is associated with ductile shearing in high Mg mafic and ultramafic metamorphic rocks. At Harmony, mineralisation is hosted within metadolerite and metabasalt. At Gruyere, mineralisation is hosted within the Gruyere Monzonite Porphyry. Gold is associated with varying intensity albite-sericite-biotite-calcite alteration of the host rock. These deposits represent significantly truncated regimes (environment D6; Figs. 2 and 4), where there is no or little locally-derived lateritic gravel. Sampling across the unconformity provided less intense but much broader geochemical

continued on page 21

Gold dispersion in transported cover sequences especially in… *continued from page 20*

targets than sampling the top of the basement. This distribution is demonstrated at Quasar, beneath 4-6 m of colluvium-alluvium (Robertson *et al*. 2001), Harmony, under 1-9 m of colluvium (Robertson *et al*. 1996) and Gruyere, under 30 m of inset-valley clays and recent colluvium-alluvium (Salama & Anand 2018b).

Pedogenic calcrete occurs mainly in the Southern region of the Yilgarn Craton, south of the Menzies Line. Gold can be enriched in carbonate horizons of soils and may give rise to, or enhance, a near-surface expression of concealed primary or secondary mineralisation (Lintern 2015). The distribution of Au is very closely correlated with Ca carbonate, commonly in the top 1–2 m of the soil; the chemical, and biogeochemical, processes involved may give surface expression even to mineralisation concealed by up to 8–10 m of transported cover.

Discussion and conclusions

Several types and ages of transported cover may overlie an *in situ* weathered profile. The interplay between Permian, Tertiary and Quaternary sedimentation and weathering have led in some places to multiple profiles, a feature described in the voluminous literature on palaeosols (Kraus, 1999). The nature and evolution of transported cover strongly influence the effectiveness of metal transfer. Mechanisms that are relevant in older (Permian, Sequence A; Eocene-Miocene, Sequence B) transported cover and climatic setting with high water tables are not relevant in Quaternary cover sequence under dry conditions. Thus, understanding the landscape history is essential to understanding the mechanisms of metal transfer and to selecting appropriate sampling media and interpreting the data.

There have been several stages of Au mobilisation in transported cover sequences. In older transported cover (Sequences A and B), in addition to mechanical dispersion, groundwater-related solubilisation and subsequent deposition of Au and pathfinder elements can form anomalies especially in Fe oxides (palaeoredox fronts) within the weathered cover at or below surface. These palaeoredox fronts occur as goethite-hematite-rich ferruginous nodules and pisoliths that are formed during the Palaeocene and more commonly Mid to Late Miocene under seasonal climatic conditions. In past saturated environments, the dispersion occurred by developing a redox gradient between the water table and buried sulphide mineralisation as proposed for electrochemical models (Govett 1976; Smee 1983; Hamilton 2000). Furthermore, the formation of stacked weathering profiles in distinct transported cover units favoured the transfer of metals across each weathering profile by bioturbation.

Although water and its dissolved constituents typically flow down-gradient, subsurface mineralised water can be transferred to the surface through faults by seismic or dilatancy pumping (Sibson *et al*. 1975). Compressional stresses along faults arising from earth tremors force the mineralised groundwaters upward, with possible surface discharge of water and their rapid evaporation resulting in near-surface anomalies (Cameron *et al*. 2002; Kelley *et al*. 2003). This is limited to low-rainfall and neo-tectonic areas that have regular seismic activity. Geochemical dispersion along ferruginised joints and fractures has been observed in the Mt Isa region of Northern Queensland (Lawrance 1999; Anand 2016; Salama *et al*. 2016b). For example, at the Osborne Cu-Au deposit where the Mesozoic transported cover is strongly faulted and fractured, the geochemical expression from the ore occurred preferentially through discrete sub-vertical fractures (Lawrance 1999; Rutherford *et al*. 2005). The country rock and palaeoredox zones host low-order anomalies close to the vertical fractures or where the redox fronts intersect the ore. However, it is not certain how much a role this mechanism has played in forming anomalies at the sites studied in Western Australia. Weathered basement at the sites investigated are commonly faulted and fractured but no vertical fractures formed by reactivation of basement faults were observed in the overlying transported cover. However, mottled, cross-laminated sandstones and siltstones with a variety of dissolution features such as dissolution-collapse brecciation are noted in the Permian cover. It is not clear whether these features are related to weathering or preferentially developed over the ore body.

The change from ferruginisation to silicification and calcification weathering is consistent with a significant decrease in rainfall and the onset of the modern dry climate. Over time, in response to this drier climate, the water table has gradually dropped to its current low position commonly between 20-30 m below surface. The association of Au with pedogenic calcrete and siliceous hardpan in Quaternary transported cover (Sequence C) indicates that movement of Au is still active. Palaeoredox fronts are not developed in recent transported cover as they were deposited when the water tables were much lower in this arid period. Mechanical with some chemical dispersion mainly occurs in the basal cover. Where it occurs, pedogenic calcrete formed in colluvium and alluvium may show an expression of mineralisation concealed by up to 10 m of transported cover. The role of plants has been demonstrated in forming anomalies in calcrete (Lintern 2015).

Our research has shown that study by microscopic analysis and micro-geochemical mapping of indicator elements in cover materials has revealed some of the mechanisms of geochemical dispersion and so indicate optimal geochemical sampling media. In older transported cover, ferruginous nodules and pisoliths and/or an unconformity between the transported cover and the underlying rock are preferred sample media. In recent transported cover, sampling of basal gravelly sediments and along the unconformity is optimal. Where it occurs, the calcrete horizon is the preferred near-surface sample medium for Au exploration, except where residual ferruginous materials are present. No other ore-related elements show this association with calcrete. More studies are needed to further identify regolith materials and minerals

continued on page 22

Gold dispersion in transported cover sequences especially in… *continued from page 21*

that might act as deep geochemical sensors of buried deposits and further provide optimal exploration sampling media for areas of deep cover.

Acknowledgements
The authors thank the numerous mining companies who have supported this research. The authors also like to thank Drs Mel Lintern, Panfeng Liu and Vasek Metelka for their help in the field and drafting some figures. Dr Louise Schoneveld is thanked for the laser ablation ICP-MS work. This paper benefitted from constructive reviews and suggestions by Drs Ian Robertson and Ryan Noble. EXPLORE referee Dr Paul Morris is thanked for his comments on an earlier version of the manuscript. Editor Beth McClenaghan is thanked for handling the manuscript.

References

Anand, R.R., Smith, R.E., Innes, J. & Churchward, H.M. 1989. *Exploration geochemistry about the Mt. Gibson Gold Deposits, Western Australia*. CSIRO Division of Exploration Geoscience, Perth, Restricted Report Number **20R** (Reissued as Open File Report **35**, CRC LEME, Perth, 1998).

Anand, R.R., Smith, R.E., Phang, C., Wildman, J.E., Robertson, I.D.M. & Munday, T.J. 1993. *Geochemical exploration in complex lateritic environments of the Yilgarn Craton, Western Australia.* CSIRO Division of Exploration Geoscience, Perth, Restricted Report, **442R** (Reissued as Open File Report **58**, CRC LEME, Perth, 1998).

Anand, R.R. 2000. Regolith and geochemical synthesis of the Yandal greenstone belt. *In*: Phillips, G.N. & Anand, R.R (eds) *Yandal Greenstone Belt*, *Australian Institute Bulletin,* **32**, 79111.

Anand, R.R. & Williamson, A. 2000. Regolith evolution and geochemical dispersion in residual and transported regolith-Calista deposit, Mt McClure district. *In*: Phillips, G.N. & Anand, R.R (eds) *Yandal Greenstone Belt*, *Australian Institute Bulletin,* **32**, 333-349.

Anand, R.R., Wildman, J.E., Varga, Z.S. & Phang, C. 2001. Regolith evolution and geochemical dispersion in transported and residual regolith-Bronzewing gold deposit. *Geochemistry: Exploration, Environment, Analysis,* **1**, 265-276.

Anand, R.R. & Paine, M. 2002. Regolith geology of the Yilgarn Craton, Western Australia: implications for exploration. *Australian Journal of Earth Sciences*, **49,** 3-162.

Anand, R.R. 2005. Weathering history, landscape evolution and implications for exploration. *In:* Anand, R.R. & de Broekert, P. (eds) *Regolith landscape evolution across Australia: A compilation of regolith landscape case studies with regolith landscape evolution models*. CRC LEME Monograph, 2-40.

Anand, R.R., Cornelius, M. & Phang, C. 2007. Use of vegetation and soil in mineral exploration in areas of transported overburden, Yilgarn Craton, Western Australia: a contribution towards understanding metal transportation processes. *Geochemistry: Exploration, Environment, Analysis*, **7**, 267-288.

Anand, R.R. & Robertson, I.D.M. 2012. Role of mineralogy and geochemistry in forming anomalies on interfaces and in areas of deep basin cover-implications for exploration. *Geochemistry: Exploration, Environment and Analysis,* **12**, 45-66.

Anand, R.R. 2015. The importance of 3D regolith-landform control in areas of transported cover implications to exploration. *Geochemistry: Exploration, Environment, Analysis,* **16**, 14-26.

Anand, R.R. 2016. Regolith-landform processes and geochemical exploration for base metal deposits in regolith-dominated terrains of the Mt Isa region, northwest Queensland, Australia. *Ore Geology Reviews,* **73**, 451-474.

Anand, R.R., Aspandiar, M.F. & Noble, R. 2016. A review of metal transfer mechanisms through transported cover with emphasis on the vadose zone within the Australian regolith. *Ore Geology Reviews,* **73**, 394-416.

Anand, R.R., Lintern, M., Hough, R., Noble, R., Verrall, V., Salama, W. & Balkau, J. 2017. The dynamics of gold in regolith change with differing environmental conditions over time. *Geology,* **45**, 127-130.

Anand, R.R., Hough, R., Salama, W., Aspandiar, M., Butt, C.R.M., Gonzalez-Álvarez, I. & Metelka, V. 2019. Gold and pathfinder elements in ferricrete gold deposits of the Yilgarn Craton of Western Australia: A review with new concepts. *Ore Geology Reviews,* **104**, 294-355.

Anon, 2009. *Tropicana Gold Project: Operational Area Groundwater Assessment*. Prepared for Anglogold Ashanti Australia Ltd and Independence Group NL. Pennington Scott.

Bagas, L. 2004. The Neoproterozoic Throssell Range and Lamil Groups, Northwest Paterson Orogen, Western Australia - A Field Guide. *Geological Survey of Western Australia. Record*, **2004/15**.

Baudet, E., Giles, D., Tiddy, C. & Hill, S. 2018. Evaluation of cover

continued on page 23

Gold dispersion in transported cover sequences especially in… *continued from page 22*

sequence geochemical exploration sample media through assessment of element migration processes. *Ore Geology Reviews*, **102**, 449-473.

Baker, P.M. 1991. *Exploration for concealed orebodies-an investigation of geochemical dispersion at Redeemer gold orebody, near Agnew, Western Australia*. WMC Report **K3409** (unpublished).

Balkau, J., French, T. & Ridges, T. 2017. Moolart Well, Garden Well and Rosedam gold deposits. *In*: Philips, G.N. (ed) *Australian Ore Deposits, The Australian Institute of Mining and Mettallurgy*, 261-266.

Bath, A.B., Miller, J., Tunijc, J., Barnes, S., Godefroy-Rodrigue, M. & Walshe, J.L. 2016. *Smokebush and Toppin Hill prospects in the context of an integrated camp-scale structural- lithogeochemical-alteration framework for the Southern Yamarna, Western Australia*. Internal CSIRO report, **58**.

Butt, C.R.M, Scott, K.M., Cornelius, M. & Robertson, I.D.M. 2005. Sample Media. *In*: Butt, C.R.M., Robertson, I.D.M., Scott, K.M. & Cornelius, M. (eds) *Regolith Expression of Ore Systems*, CRCLEME, 2005, 53-79.

Cameron, E.M., Leybourne, M.I. & Kelley, D.L. 2002. Exploring for deeply covered mineral deposits: formation of geochemical anomalies in northern Chile by earthquake-induced surface flooding of mineralized groundwaters. *Geology,* **30**, 1007-1010.

Carver, R., Baker, P. & Oates, C. 2005. Redeemer gold deposit, Agnew district, WA. *In*: Butt, C.R.M., Robertson, I.D.M., Scott, K.M. & Cornelius, M. (eds) *Regolith Expression of Ore Systems*, CRCLEME, 2005, 320-322.

de Broekert, P. & Sandiford, M. 2005. Buried inset-valleys in the Eastern Yilgarn Craton, Western Australia: geomorphology, age and allogenic control. *Journal of Geology,* **113**, 471-493.

Doyle, M.G., Catto, B., Gibbs, D., Kent, M. & Savage, J. 2017. Tropicana gold deposit. *In*: Phillips, G.N. (ed) *Australian Ore Deposits, the Australian Institute of Mining and Metallurgy*, 299-306.

Eyles, N. & de Broekert, P. 2001. Glacial tunnel valleys in the Eastern Goldfields of Western Australia cut below the Late Paleozoic Pilbara ice sheet. *Palaeogeography Palaeoclimatology Palaeoecology,* **171**, 29-40.

Gallant, J.C. & Dowling, T.I. 2003. A multiresolution index of valley bottom flatness for mapping depositional areas. *Water Resources Research,* **39**.

Geoscience Australia, 2009. *Digital Elevation Model of Australia. SRTM-derived 1 Second Digital Elevation Models Version 1.0*. <http://www.ga.gov.au/scientific-topics/national-location-information/digital-elevation-data>.

Govett, G.J.S. 1976. Detection of deeply buried and blind sulphide deposits by measurement of H^+ and conductivity of closely spaced surface soil samples. *Journal of Geochemical Exploration*, **6**, 359-382.

Hallberg, J.A. 1984. A geochemical aid to igneous rock identification in deeply weathered terrains. *Journal of Geochemical Exploration*, **20**, 1-8.

Hill, S. M. 2004, Biogeochemical sampling media for regional- to prospect-scale mineral exploration in regolith-dominated terrains of the Curnamona Province and adjacent areas in western NSW and eastern SA. *In*: *Proceedings of the CRC LEME Regional Regolith Sympoisa*, November 2004, Perth, WA, 128-133.

Hamilton, S.M. 2000. Spontaneous potentials and elctrochemical cells. *In:* Hale, M. (ed) *Geochemical Remote Sensing of the Subsurface*, **7**, Elsevier, Amsterdam, 421-42. Hore, S.B. & Hill, S.M. 2009. Palaeoredox fronts: setting and associated alteration exposed within a key section for understanding uranium mineralisation at the Four Mile West deposit. *Mesa Journal* **55**, 34-39.

Hronsky, J.M.A., Perriman, R.P.A. & Schmulian, M.L. 1990. Lancefield Gold deposit, Laverton. *In:* Hughes, F.E. (ed) *Geology of the Mineral Deposits and Papua and New Guinea*, 511-517 (AUSIMM: Melbourne).

Hulme, K.A. & Hill, S.M. 2005. River red gums as an important biogeochemical sampling media for mineral explorers and environmental chemists. *In*: *22nd International Geochemical Exploration Symposium*, Perth, 59-60.

Kelley, D.L., Hall, G.E.M., Closs, L.G., Hamilton, I.C. & McEwen, R.M. 2003. The use of partial extraction geochemistry for copper exploration in northern Chile. *Geochemistry: Exploration, Environment, Analysis,* **3**, 85-104.

Kern, A.M. & Commander, P. 1993. Cainozoic stratigraphy in the Roe Palaeodrainage of the Kalgoorlie region, Western Australia. *Geological Survey of Western Australia Professional Paper*, 85-95.

Kraus, M. 1999. Paleosols in clastic sedimentary rocks: their genetic applications. *Earth Science Reviews*, **47**, 41-70.

Lawrance, L.M. 1999. Multi-element dispersion in Mesozoic basin sediment over the Osborne Deposit, northern Queensland, Australia: Implications for regional geochemical exploration in buried terrain. *Australian Institute of Geoscientists Bulletin*, **28**, 73-81.

Lintern, M., Anand, R.R., Hough, R., Shaw, D. & Pinchand, T. 2009. *Biogeochemical and regolith investigations at Tropicana gold deposit, Western Australia*. CSIRO Report **P2009**.

Lintern, M., Anand, R.R., Ryan, C. & Paterson, D. 2013a. Natural gold particles in Eucalyptus leaves and their relevance to exploration for buried gold deposits. *Nature Communications.* **4,** 1-7.

Lintern, M., Anand, R.R. & Reid, N. 2013b. *Exploration geochemistry at Garden Well Gold Deposit NE Yilgarn Craton (Western Australia)*. CSIRO Report No **EP1310007**.

Lintern, M.J. 2015. The association of gold in calcrete. *Ore Geology Reviews,* **66**, 132-199.

Mann, A.W. 1983. Hydrogeochemistry and weathering on the Yilgarn Block, Western Australia-ferrolysis and heavy metals of continental brines. *Geochimica et Cosmochimica Acta*, **47**, 181-190.

McGowran, B. & Li, Q. 1998. Cainozoic climate change and its implications for studying the Australian regolith. *In*: Eggleton, R.A. (ed) *The State of the Regolith. Geological Society of Australia, Special Publication*, **20**, 86-103.

Martin, H.A. 2006. Cenozoic climatic change of arid vegetation in Australia. *Journal of Arid Environment,* **66**, 533-563.

Myers, J.S. 1993. Precambrian history of the West Australian Craton and adjacent orogens. *Annual Review of Earth and Planetary Sciences*, **21**, 453-481.

Noble, R.R.P., Anand, R.R., Gray, D. & Cleverley, J. 2017. Metal migration at the DeGrussa Cu-Au sulphide deposit, Western Australia. *Geochemistry: Exploration, Environment, Analysis,* **17**, 124-142.

Noble, R.R.P., Lau, I.C., Anand, R.R. & Pinchand, T. 2019. *Multi-scaled near surface exploration using ultrafine soils*. Geological Survey of Western Australia Report **190**.

continued on page 24

Gold dispersion in transported cover sequences especially in… *continued from page 23*

Parker, A. 1970. An index of weathering for silicate rocks. *Geological Magazine,* **107**, 501-504.

Petts, A.E., Hill, S.M. & Worrall, L. 2009. Termite species variations and their importance for termitaria biogeochemistry: Towards a robust media approach for mineral exploration. *Geochemistry: Exploration, Environment, Analysis,* **9**, 257-266.

Pidgeon, R. T., Brander, T. & Lippolt, H.J. 2004**.** Late Miocene (U+Th)–He ages of ferruginous nodules from lateritic duricrust, Darling Range, Western Australia. *Australian Journal of Earth Sciences,* **51**, 901-909.

Pillans, B. 2005. Geochronology of the Australian regolith. *In*: Anand, R.R. & de Broekert, P. (eds) *Regolith Landscape Evolution Across Australia*, CRC LEME, Perth, 41-61.

Price, J.R. & Velbel, M.A. 2003. Chemical weathering indices applied to weathering profiles developed on heterogeneous felsic metamorphic parent rocks. *Chemical Geology*, **202**, 397-416.

Radford, N.W. & Burton, P.E. 1999. The geochemistry of transported overburden: the time factor. An example from Fender deposit, Big Bell, Western Australia. *Journal of Geochemical Exploration*, **66**, 71-83.

Reid, N., Hill S.M. & Lewis, D.M. 2008. Spinifex biogeochemical expressions of buried gold mineralisation: the great mineral exploration penetrator of transported regolith. *Applied Geochemistry*, **23**, 76-84.

Robertson, I.D.M., Phang, C. & Munday, T.J. 1996. *The regolith geology and geochemistry of the area around the Harmony Gold Deposit, (Baxter Mining Centre), Peak Hill, Western Australia*. CSIRO Exploration and Mining Restricted Report **194R** (Reissued as Open File Report **94**, CRC LEME, Perth, 2001).

Robertson, I.D.M., King, J.D. & Anand, R.R. 2001. Regolith geology and geochemical exploration around the Stellar and Quasar gold deposits, Mt Magnet, Western Australia. *Geochemistry: Exploration, Environment, Analysis*, **1**: 353-365.

Rutherford, N.F., Lawrance, L.M. & Sparks, G. 2005. Osborne Cu-Au deposit, Cloncurry district, Northwest Queensland. *In*: Butt, C.R.M., Robertson, I.D.M., Scott, K.M. & Cornelius, M. (eds) *Regolith Expression of Australian Ore Systems*, CRC LEME, Perth, 380-382.

Salama, W., Anand, R.R. & Verrall, M. 2016a. Mineral exploration and basement mapping in areas of deep transported cover using indicator heavy minerals and paleoredox fronts, Yilgarn Craton, Western Australia. *Ore Geology Reviews,* **72**, 485-509.

Salama, W., Gazley, M.F. & Bonnett, L.C. 2016b. Geochemical exploration for supergene copper oxide deposits, Mount Isa Inlier, NW Queensland, Australia. *Journal of Geochemical Exploration,* **168**, 72-102.

Salama, W. & Anand, R.R. 2017. Reconstructing the pre-Quaternary landscape in Agnew-Lawlers area, Western Australia with emphasis on the Permo-Carboniferous glaciation and post-glacial weathering. *International Journal of Earth Sciences,* **106**, 311-339.

Salama, W. & Anand, R.R. 2018a. Ferruginous pisoliths as a powerful regolith sampling medium for exploring areas covered by sand dunes. Gold 18@Perth, *Australia Institute of Geoscientists*, Abstract Volume, 53-54.

Salama, W. & Anand, R.R. 2018b. *Regolith-landform evolution and geochemical exploration through transported cover at Yamarna Terrane, Western Australia*. CSIRO Mineral Resources report, **E181939**, Perth, Australia.

Sibson, R.H., Moore, J.M. & Rankin, A.H. 1975. Seismic pumping, a hydrothermal fluid transport mechanism. *Journal of Geological Society London*, **131**, 653-659.

Smee, B.W. 1983. Laboratory and field evidence in support of the electrogeochemically enhanced migration of ions through glaciolacustrine sediment. *Journal of Geochemical Exploration*, **19**, 277-304.

Spaggiari, C.V., Bodorkos, S., Barquero-Molinna, M., Tyler, I.M. & Wingate, M.T.D. 2009. Interpreted bedrock geology of the South Yilgarn, and central Albany-Fraser Orogen, Western Australia. *Geological Survey of Western Australia Record **2009/10***.

Stewart, A.D., Anand, R.R. & Balkau, J. 2012. Source of anomalous gold concentrations in termite nests, Moolart Well, Western Australia: Implications for exploration. *Geochemistry: Exploration, Environment, Analysis*, **12**, 327–337.

Stewart, A.D. & Anand, R.R. 2014. Anomalies in insect nest structures at the Garden Well gold deposit: Investigation of mound-forming termites, subterranean termites and ants. *Journal of Geochemical Exploration*, **140**, 77–86.

Veevers, J.J. 2000. *Billion-year Earth History of Australia and Neighbours in Gondwanaland: Sydney*. Geomoc Press.

Wells, M., Danisik, M. & McInnes, B. 2018. (U-Th)/He dating of ferruginous duricrust, Boddington gold mine, Western Australia. *Geological Survey of Western Australia Record **2018/13.***